Reliability testing for product return prediction

Zhao, Xiujie; Chen, Piao; Lv, Shanshan; He, Zhen

DOI
10.1016/j.ejor.2022.05.012

Publication date
2023

Document Version
Final published version

Published in
European Journal of Operational Research

European Journal of Operational Research 304 (2023) 1349–1363

Contents lists available at ScienceDirect

European Journal of Operational Research

journal homepage: www.elsevier.com/locate/ejor

Interfaces with Other Disciplines

Reliability testing for product return prediction

Xiujie Zhao[a], Piao Chen[b,*], Shanshan Lv[c], Zhen He[a]

[a] College of Management and Economics, Tianjin University, Tianjin, China
[b] Department of Applied Mathematics, Delft University of Technology, Delft, the Netherlands
[c] School of Economics and Management, Hebei University of Technology, Tianjin, China

ARTICLE INFO

Article history:
Received 17 August 2021
Accepted 7 May 2022
Available online 13 May 2022

Keywords:
Reliability
Accelerated degradation test
Fisher information
Optimal design
Warranty prediction

ABSTRACT

Return of products within the warranty coverage induces additional cost and loss of reputation to manufacturers. It is of practical interest to predict the return rate by experimental means before introducing a product to the market. In this paper, we propose to optimize accelerated reliability tests to achieve the goal within limited time. To describe the heterogeneity in the customers' usage mode, a discrete random variable is employed to model the degradation rate in addition to the continuous stress variable. To further characterize the heterogeneity in the customers' behavior, two models of product return are investigated: one assumes that customers return products once the degradation level reaches the minimum eligible return threshold and the other assumes that the threshold varies among different customers. Optimal reliability tests are planned under the large-sample assumption with two novel test schemes: global optimal planning and stress constrained planning. Insights regarding the optimal plans are gleaned to ameliorate the test planning procedure and verify the optimality. A real example from the battery industry is then presented along with the simulation study and sensitivity analysis to demonstrate the methods. We find that the randomness in return level results in different test plans. Furthermore, the constrained optimal plans offer more robustness to the compromise plans.

1. Introduction

1.1. Background and motivation

Manufacturers are putting more effort in enhancing product reliability to attain competitiveness in the market. Nowadays, most products are sold with warranty, which acts as a contractual obligation by manufacturers to provide free or discounted after-sale service upon the product failure or malfunction under a specific coverage policy. During the warranty coverage period, the product return rate is one of the most representative measures that reflect the reliability performance under certain warranty policies. A high return rate within warranty coverage usually incurs reduced sales of products and poor reputation to the manufacturer (Walsh, Albrecht, Kunz, & Hofacker, 2016), in addition to the immediate increase in maintenance/replacement cost, which could account for a remarkable proportion of the operational cost of a manufacturer. Therefore, to control the return rate is essential to extract more profit from customers and establish positive marketing influences and reputation.

With the rapid emergence of new products, it is of great importance to predict the return rate for products free of tracking history (Darghouth, Ait-kadi, & Chelbi, 2017). The evaluation of future warranty claims under usage condition can be realized indirectly via reliability tests. Some realistic constraints attach challenges to the prediction problems. Manufacturers usually wish to shorten the duration of reliability tests. To achieve this goal, accelerated-stress reliability tests are preferred, yet extrapolation is inevitable for accelerated tests. Further, the usage mode usually varies among sold products due to different customers' behaviors. Variable usage modes not only influence the expected return rate, but also augment the variability in return rate prediction.

A typical example of this type is the rechargeable battery. Battery manufacturers test the battery capacity over time prior to their introduction to the market. Many rechargeable batteries are returned due to unsatisfactory capacity within the warranty coverage. Battery capacity is believed to decrease over time and the deterioration can be accelerated by several factors (Li, Rezvanizaniani, Ge, Abuali, & Lee, 2015). Specifically, temperature is deemed to make the most significant effects, therefore, battery manufacturers usually set operating ambient temperature at a specified range to avoid irreversible damages to the batteries. Moreover, consumers behaviors, such as the selection of recharging and discharging

* Corresponding author.
E-mail addresses: xiujiezhao@tju.edu.cn (X. Zhao), p.chen-6@tudelft.nl (P. Chen).

https://doi.org/10.1016/j.ejor.2022.05.012

modes, may also influence the speed of battery capacity degradation. Behind the huge success of e-commence in China, there exist numerous delivering vehicles of which the quantity keeps increasing rapidly. These vehicles are mostly equipped with rechargeable batteries, and they are used under various usage habits. In the presence of the aforementioned sources of variability, the reliability tests need to be carefully planned to obtain as much useful information as possible for the prediction of product return rate. Unlike conventional accelerated tests designed to estimate the mean-time-to-failure (MTTF) or life quantiles, the aims of reliability tests for return rate prediction lie in two aspects: a) to accurately estimate the proportion of returned products in population; b) to better understand the relationship between product degradation and covariates in usage condition and mode, and thereby assist decision makers to specify usage instructions. Motivated by the battery example, in this paper, we address the general planning of reliability test under multiple experimental factors for return rate prediction.

1.2. Related works

Sitting in the interface of design of reliability experiments (tests) and warranty analysis, our work mainly deals with the problem of reliability test planning for return rate prediction within the warranty coverage. To this end, we give literature review on the following related topics.

Modeling of accelerated degradation tests. From a broader view of classification, accelerated reliability tests consist of life tests and degradation tests. Owing to the utilization of dynamic measurable quality characteristics, accelerated degradation tests (ADT) have shown great advantages over accelerated life tests (ALT) after the enlightening work by Meeker, Escobar, & Lu (1998), especially for highly reliable products (Fang, Pan, & Wang, 2022; Wang, Wang, Hong, & Jiang, 2021; Ye & Xie, 2015). In an ADT, test units are exposed to elevated stresses to increase their degradation rates. As a compensation for the inevitable extrapolation in estimation, the accelerated stresses can considerably shorten the test duration. ADT has been widely investigated and applied in the battery industry. Thomas, Bloom, Christophersen, & Battaglia (2008) utilized ADT data to predict the life of lithium-ion cells with general path models. In Cheng, Li, Yuan, Zhang, & Liu (2016), nonlinear curve fitting methods were proposed to predict the lifetime for lithium thionyl chloride batteries via ADT data. Li et al. (2015) treated a NASA battery dataset as the historical data and employed a simulated Bayesian approach to plan the step-stress ADT. Further, random fuzzy model was formulated to characterize the random effects in time dimension and unit-unit variations and the method was applied to the lithium-ion battery (Li, Wu, Ma, Li, & Kang, 2018). Current studies commonly regard temperature, charging and discharging voltage/current as key factors that affects the battery capacity over time (Zhu et al., 2020). In addition, many existing works have contributed to the degradation modeling for rechargeable batteries without accelerated stress conditions (Si, 2015; Ye & Chen, 2014; Zhai & Ye, 2017).

Warranty analysis via experimental results. Although a large amount of effort has been put into degradation data analysis and degradation tests, the research concerning the linkage between warranty issues (e.g., return rate, warranty cost, warranty policy) and experimental tests is relatively scant. Most extant works predominately adopt life models for warranty analysis and overlook the degradation models. Yang (2010) optimized ALT plans to minimize the asymptotic variance of predicted warranty cost under a replacement policy. Zhao & Xie (2017) and Zhao, He, & Xie (2018) utilized ALT and ADT data to predict the number of warranty claims with a fixed period under environmental variation, respectively. In Hsu, Tseng, & Chen (2015) and Tseng, Hsu, & Lin (2016), Bayesian framework was employed to jointly model field return date and lab data for warranty prediction. While one can witness the initial emergence of related works, these studies have not zoomed into the reliability test planning problem with multiple covariates that can be either continuous or discrete.

Optimization of accelerated test plans. The most widely used paradigm for accelerated reliability test planning is to utilize the asymptotic property of maximum likelihood estimators (MLEs). Under the large-sample assumption, the Fisher information of unknown parameters can well characterize the estimation uncertainty (Meeker & Escobar, 2015). In this sense, the uncertainty in desired estimation can be inferred via the classic delta method. In the context of degradation tests, where more informative data can be collected than in life tests, the appropriateness of the large-sample approximation is usually well justified. More advanced approaches have been intensely explored on this mainstream direction of optimization to improve the applicability and robustness of test plans. To name a few, Zhang & Meeker (2006) employed a Bayesian method to maximize the pre-posterior utility and obtain the robust optimal ALT plan under model uncertainty. To enhance the generality of ADT planning approaches, Lee, Tseng, & Hong (2020) proposed an exponential-dispersion degradation model that generalize commonly used stochastic models and provided the closed-form ADT plans. The studies mentioned above all deal with the asymptotic properties of the objective function. Such methods are proved to be reasonably accurate by simulation studies. Most existing studies identify the minimization of asymptotic variance of key reliability characteristics, such as the mean time to failure (MTTF) and life quantiles, as their criteria. To the best of our knowledge, the criterion that concerns the prediction of return rate, is still underexplored.

1.3. Overview

This paper prescribes an ADT planning method for return rate prediction under one continuous quantitative factor and one qualitative factor. Potential inherent correlation between the two factors is addressed in the test planning phase. Further, the heterogeneity in the customers usage mode is taken into consideration to achieve more accurate prediction. In view of practical assumptions, we inaugurate new criteria of optimal plans for two different return models. The criteria of optimality are established based on the large-sample approximation. In addition, two test schemes are put forward for different application scenarios. To the best of our knowledge, the work sheds new lights on the reliability testing research by being the first to simultaneously address the following issues:

1. We propose a novel criterion of optimality that concerns the return rate prediction for accelerated tests. The criterion intend to aid decision makers to predict the proportion of returned products in the design phase
2. We put forward a framework to plan accelerated tests in the presence of both continuous and discrete factors. Specifically, we construct the optimal test plans for degrading products in the presence of both the continuous environmental stress and multiple usage modes.
3. The proposed model enables the randomness in the degradation level of the returned product, which is quite common in practice. In addition, we provide rigorous evaluations approaches to the return rate in the presence of the aforementioned randomness.
4. We introduce two test schemes: global optimal plans and constrained optimal plans to enhance the generality of proposed methods. Global optimal plans can achieve the most accurate prediction, whereas constrained optimal plans pro-

vide feasible options to manufacturers with limited test chambers.

The paper proceeds as follows. Section 2 presents the return rate modeling under the Wiener degradation process. In Section 3, the approaches to test plan optimization are detailed, based on which we provide some general insights to test planners. Section 4 demonstrates the proposed methods systematically with a practical example, in which we also carry out simulation studies and sensitivity analysis to illustrate the robustness of optimal plans. Conclusions are drawn in Section 5. Technical proofs are relegated in the Appendix A.

2. Modeling of return rate under degradation models

2.1. Wiener degradation process with covariates

The Wiener process has been successfully applied to model the degradation of rechargeable batteries due to the fact that the degradation paths of batteries are oftentimes non-monotone (Si, 2015; Zhang, Si, Hu, & Lei, 2018). In the paper, we use the Wiener process as the degradation model and it can be easily extended to other stochastic processes for the adaptation to other products/systems. Under a covariate vector denoted by $\boldsymbol{x}_0$, the degradation process $Y(t|\boldsymbol{x}_0)$ is given as follows:

$$Y(t|\boldsymbol{x}_0) = y_0 + \mu(\boldsymbol{x}_0)\Psi(t) + \sigma\mathcal{B}(\Psi(t)), \qquad t \geq 0, \tag{1}$$

where y_0 is the initial degradation level, $\mu(\boldsymbol{x}_0)$ is the drift parameter evaluated at $\boldsymbol{x}_0$, $\Psi(t)$ is the time scale function to characterize the nonlinearity in degradation path, σ is the diffusion parameter, and $\mathcal{B}(\cdot)$ is the standard Brownian motion. Standing on the model in (1), covariates regarding usage condition $\boldsymbol{x}_0$ exert influences on the drift properties of the degradation paths, and the volatility stays constant over any $\boldsymbol{x}_0$. Note that the assumption has been commonly made and verified by extant works (Hu, Lee, & Tang, 2015; Lim & Yum, 2011). Without loss of generality, $\Psi(t) = t$ is assumed to imply a linear degradation path under a fixed $\boldsymbol{x}_0$ for simplicity. Further, we divide $\boldsymbol{x}_0$ into two parts by $\boldsymbol{x}_0 = \left(\boldsymbol{x}_0^{(1)}, \boldsymbol{x}_0^{(2)}\right)$, where $\boldsymbol{x}_0^{(1)}$ and $\boldsymbol{x}_0^{(2)}$ represent the continuous quantitative variables and discrete qualitative variables, respectively.

For the better exposition of the proposed methods, we consider the scenario in which there is one continuous quantitative factor and one discrete qualitative factor in $\boldsymbol{x}_0$, which we denote by $\boldsymbol{x}_0 = (x_0, m_0)$. It is worth mentioning that the proposed framework can be readily extended to consider more factors (Fang, Pan, & Stufken, 2020). For rechargeable batteries, x_0 usually represents a transformed variable of the environmental temperature, which is believed to be a dominating factor affecting the battery capacity (Tian, Xiong, & Shen, 2020). In contrast, the discrete factor m_0 cannot be quantified or ordered. In the context of the battery example, the factor could characterize the recharging and discharging mode of the battery. To characterize the heterogeneity in the usage mode, we assume that m_0 has M categories, and m_0 is characterized by a discrete random distribution. For $m = 1, \ldots, M$, a value ρ_m is assigned to quantify the probability that customers use the product under mode $m_0 = m$, i.e., $\Pr(m_0 = m) = \rho_m$. Let $\boldsymbol{\rho} = (\rho_1, \ldots, \rho_M)$, and $\boldsymbol{\rho}$ can be estimated via customer survey and records of similar products from the manufacturer. **R**emark Since factors like the usage mode cannot be modeled as continuous variables or even ordinal discrete variables, we can only model them as discrete random variables and employ the probability mass to characterize them. In practice, a customer may use the product with modes that vary over time. We can employ a deterministic function, or, more generally, a stochastic process to characterize the usage mode as $M_0(t)$. The main challenge in modeling the problem with time-varying usage mode lies in the derivation of the reliability function when $M_0(t)$ is stochastic. Simulation-based methods can be resorted to if the reliability function cannot be derived analytically. In this work, for simplicity, we can regard $M_0(t)$ as a controlled variable and assume that it is constant over time in the ADT. By considering all the usage modes in the test planning, the results obtained from the proposed method can be easily utilized to predict the return rate if the usage mode is time varying.

2.2. Degradation under accelerated tests

Accelerated tests are conducted under elevated stresses in comparison to usage conditions. A common exercise to test products is to expose them in moderately higher temperatures. Next, we denote the degradation rate under $\boldsymbol{x}_m = (x, m)$ by $\mu(x, m) = \mu(\boldsymbol{x}_m)$. Following previous literature of reliability tests, the standardized quantitative factor x is a variable between 0 and 1, which satisfies that $x_0 \equiv 0$ and $x_{\max} = 1$. Further, we assume that the degradation rate can be modeled by the well-known log-linear function (Zhang & Meeker, 2006), while different from existing models, we propose a multivariate model are as follows:

$$\log\mu(x, m) = \begin{cases} \beta_0 + \beta_1 x, & \text{if } m = 1, \\ \beta_0 + \beta_m x + \gamma_m, & \text{if } m = 2, \ldots, M, \end{cases} \tag{2}$$

for $x \in [0, 1]$ and $m = 1, \ldots, M$. In the model, the parameter set $\{\beta_m, m = 1, \ldots, M\}$ characterizes the effect of the continuous factor under different m, while $\{\gamma_m, m = 1, \ldots, M\}$ characterizes the effect of the discrete factor that is independent of the continuous factor. Since we have used β_0 to benchmark the log-degradation-rate given that $x = 0$ and $m = 1$, it is set that $\gamma_1 \equiv 0$. The model can characterize the effects of both the continuous and discrete factors, as well as their mutual interactions by assigning a different β to each x under a specific m. Under the current model, the unknown parameters are denoted by $\boldsymbol{\theta} = (\beta_0, \beta_1, \ldots, \beta_M, \sigma, \gamma_2, \ldots, \gamma_M)'$. Here, we note that only the continuous factor is accelerated in the test. Moreover, since x is standardized to 0 at usage condition, the extrapolation to predict field reliability at $x_0 = 0$ only involves parameters β_0, σ and $\gamma_2, \ldots, \gamma_M$.

Remark 1. The log-linear model has been widely adopted in the existing works on ALT/ADT planning and analysis (Escobar & Meeker, 2006; Ye & Xie, 2015). An appealing advantage of the model is its flexibility to characterize different types of physical/-chemical acceleration relationships, including the Arrhenius relationship that considers temperature, Peck relationship that considers both temperature and humidity and the power law relationship that incorporates factors such as voltage and current. Therefore, the proposed methods can be readily used to plan accelerated tests for products with various factors, besides rechargeable batteries.

2.3. Return rate prediction under heterogeneous usage mode - a basic model

The return rate of products is determined by both the inherent reliability properties and external usage conditions and modes. Without loss of generality, we assume that $y_0 \equiv 0$ in (1). We first elaborate a simple and ideal scenario under which a customer definitely returns the sold product if its degradation level exceeds a fixed failure threshold L. Let T be the return time from the product purchase and it is the equivalent random variable as the failure time implied by the current assumption. Under a fixed warranty coverage period τ_W and usage condition $\boldsymbol{x}_0 = (x_0, m)$, the product return rate, denoted by $P_R(\tau_W, \boldsymbol{x}_0; \boldsymbol{\theta}, L)$, is equal to the unreliability at τ_W, that is,

$$P_R\left(\tau_W, \boldsymbol{x}_0; \boldsymbol{\theta}\right) = 1 - R\left(\tau_W; \boldsymbol{x}_0, \boldsymbol{\theta}\right) = F_T\left(\tau_W; \boldsymbol{x}_0, \boldsymbol{\theta}, L\right), \tau_W \geq 0 \tag{3}$$

where $R(\cdot)$ and $F_T(\cdot)$ are the reliability function and cumulative distribution function (CDF) of the failure time, respectively. Under the Wiener degradation model, the failure time T is defined as the first passage time to the failure threshold L, i.e., $T = \inf\{t; Y(t|\boldsymbol{x}_0) \geq L\}$. It is well known that T follows an inverse Gaussian (IG) distribution with mean $L/\mu(\boldsymbol{x}_0)$ and shape L^2/σ^2 (Chhikara, 1988), and the CDF evaluated at any $\tau_W > 0$ is given by

$$F_T\left(\tau_W; \boldsymbol{x}_0, \boldsymbol{\theta}, L\right) = \Phi\left[\sqrt{\frac{1}{\sigma^2\tau_W}}(\mu(\boldsymbol{x}_0)\tau_W - L)\right] + \exp\left[\frac{2\mu(\boldsymbol{x}_0)L}{\sigma^2}\right] \Phi\left[-\sqrt{\frac{1}{\sigma^2\tau_W}}(\mu(\boldsymbol{x}_0)\tau_W + L)\right], \quad (4)$$

where $\Phi(\cdot)$ is the CDF of the standard normal distribution. Taking into account the heterogeneity in the discrete factor, the overall expected product return rate (EPRR) under L is given by taking the expectation of $P_R(\tau_W, \boldsymbol{x}_0; \boldsymbol{\theta}, L)$ with respect to M_0:

$$\mathrm{EPRR}_0(L) = \mathbb{E}_{M_0}\left[P_R(\tau_W, \boldsymbol{X}_0; \boldsymbol{\theta})\right] = \sum_{m=1}^{M} \rho_m F_T\left(\tau_W; (x_0, m), \boldsymbol{\theta}, L\right), \quad (5)$$

for $L > 0$. With given parameters and L, the overall return rate is convenient to evaluate as $F_T(\cdot)$ has a typical form of an inverse Gaussian CDF. Recall that a predominant assumption in the subsection is that all customers return products at threshold L, which is sometimes impractical in the real market. In the next subsection, we relax the assumption to enhance the flexibility of the return model.

2.4. Return rate prediction under heterogeneous usage mode: A random returning model

A natural practice of product return is that a customer is more likely to return the product when the degradation level is higher. On the one hand, manufacturers usually set a minimum degradation level that is eligible for product return. For instance, battery providers may follow the policy that batteries with a capacity 80% or less are eligible for return within the warranty contract, otherwise free-of-charge replacement/repair cannot be guaranteed. On the other hand, not all customers would return their purchases immediately when the products reach the returnable status. More often than not, there is a random gap between the minimum returnable level and actual level upon the return. It is noteworthy that there already exists literature that addresses the reliability modeling for Wiener degradation models under random failure thresholds. For some recent contributions, one can be referred to Wang & Coit (2007), Hua, Zhang, Xu, Zhang, & Xu (2013), Sarada & Shenbagam (2021) and Li, He, & Zhao (2022). To characterize the randomness in the return model, we introduce one fixed threshold $l_{\min}$ and one positive random variable $L_D > 0$ to represent the minimum returnable degradation level and the difference between the actual return level and $l_{\min}$, respectively. It is obvious that the actual return level is $l_{\min} + L_D$.

The involvement of L_D improves the applicability of the model by capturing customers' behaviors more realistically. However, this creates a hurdle to evaluate the return rate because T no longer follows a known distribution in presence of the random effect. We put forth two different approaches to obtain the CDF of T to facilitate the calculation of return rate: an exact characteristic function-based method and a first-order approximated method. First, suppose that a fixed $l_{\min}$ is given and L_D follows a known continuous distribution with characteristic function $\varphi_{L_D}(z)$. We have the following proposition that gives the EPRR.

Proposition 1. *The EPRR can be exactly evaluated by the following function:*

$$\mathrm{EPRR}_1(l_{\min}, L_D) = \sum_{m=1}^{M} \rho_m \check{F}_T\left(\tau_W; (x_0, m), \boldsymbol{\theta}, l_{\min} + L_D\right), \quad (6)$$

and

1. *T follows a distribution with the following characteristic function:*

$$\varphi_T(z) = \int_0^{\infty} \exp\left[\frac{(l_{\min} + L_D)\mu(x_0, m)}{\sigma^2}\left(1 - \sqrt{1 - \frac{2\sigma^2 iz}{\mu(x_0, m)^2}}\right)\right] f_{L_D}(l)dl. \quad (7)$$

2. *The CDF $\check{F}_T\left(\tau_W; (x_0, m), \boldsymbol{\theta}, l_{\min} + L_D\right)$ is given by*

$$\check{F}_T\left(\tau_W; (x_0, m), \boldsymbol{\theta}, l_{\min} + L_D\right) = \frac{1}{2} - \frac{1}{\pi}\int_0^{\infty} \frac{\mathrm{Im}\left[e^{-iz\tau_W}\varphi_T(z)\right]}{z} dz, \quad (8)$$

where $\mathrm{Im}(\cdot)$ *is the imaginary part of a complex number.*

The proposition is a ready result in light of the theorems in Gil-Pelaez (1951). Following the proposition, the EPRR can be computed exactly with the aid of characteristic functions. However, the computation of (8) may be onerous under certain distributions of L_D. Alternatively, we can resort to approximated methods that are more tractable to evaluate. The following proposition provides an approximation to EPRR via the Taylor series:

Proposition 2. *The EPRR can be approximately evaluated by*

$$\mathrm{EPRR}_2(l_{\min}, L_D) = \sum_{m=1}^{M} \rho_m \mathbb{E}_{L_D}\left[F_T\left(\tau_W; (x_0, m), \boldsymbol{\theta}, l_{\min} + L_D\right)\right], \quad (9)$$

if we regard

$$\mathbb{E}_{L_D}[F_T(\mu_{L_D} + l_{\min})] \approx \mu_{L_D} + \frac{1}{2}F_T^{(2)}(\mu_{L_D} + l_{\min})\mathrm{var}(L_D), \quad (10)$$

where μ_{L_D} is the mean of random variable L_D. If we denote the density function of the standard normal distribution by $\phi(\cdot)$, $F_T^{(2)}\left(\mu_{L_D} + l_{\min}\right)$ is given by:

$$F_T^{(2)}(\mu_{L_D} + l_{\min}) = A\phi\left[\left(\frac{1}{\sigma^2\tau_W}\right)^{1/2}(\mu(\boldsymbol{x}_0)\tau_W - l_{\min} - \mu_{L_D})\right] + B\Phi\left[-\left(\frac{1}{\sigma^2\tau_W}\right)^{1/2}(\mu(\boldsymbol{x}_0)\tau_W + l_{\min} + \mu_{L_D})\right] + C\phi\left[-\left(\frac{1}{\sigma^2\tau_W}\right)^{1/2}(\mu(\boldsymbol{x}_0)\tau_W + l_{\min} + \mu_{L_D})\right], \quad (11)$$

and

$$A = -\left(\frac{1}{\sigma^2\tau_W}\right)^{3/2}(\mu(\boldsymbol{x}_0)\tau_W - l_{\min} - \mu_{L_D}),$$

$$B = \frac{4\mu^2(\boldsymbol{x}_0)}{\sigma^4}\exp\left[\frac{2\mu(\boldsymbol{x}_0)(l_{\min} + \mu_{L_D})}{\sigma^2}\right],$$

$$C = \left[\left(\frac{1}{\sigma^2\tau_W}\right)^{3/2}(\mu(\boldsymbol{x}_0)\tau_W + l + \mu_{L_D}) - \frac{4\mu(\boldsymbol{x}_0)}{\sigma^2}\left(\frac{1}{\sigma^2\tau_W}\right)^{1/2}\right] \exp\left[\frac{2\mu(\boldsymbol{x}_0)(l_{\min} + \mu_{L_D})}{\sigma^2}\right].$$

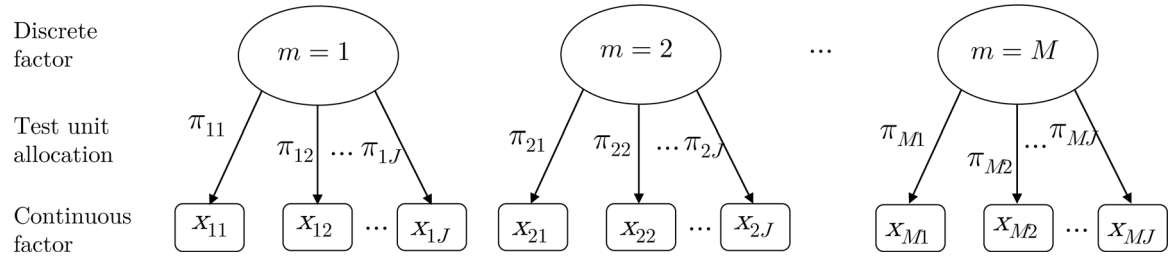

Fig. 1. Illustration of the ADT planning.

As a side note, the selection of distribution for L_D is sort of an open question to decision makers. The distribution of L_D can reflect different customers' behaviors. For example, if one wants to describe the scenario in which the customers are more sensitive to the degradation performance, it can be assumed that L_D follows a distribution with relatively large density at values that are closer to 0. Meanwhile, it is also possible that a significant delay exists and makes the mode of L_D greater than 0. Fortunately, manufacturers usually own previous warranty claim data to facilitate the modeling of L_D, either from the same type of products or similar products. Decision makers may fit known distributions to the data and compare the fitness. Since the topic is well established in the statistical literature and is not the main focus of the paper, we skip more detailed discussions.

3. Reliability test planning

In this section, test planning approaches to predict return rate are presented. Section 3.1 introduces the notations and preliminaries regarding the test. Section 3.2 prescribes two types of planning from practical perspectives. In Section 3.3 and 3.4, general insights are gleaned.

3.1. Preliminaries

Unlike conventional one-factor problems, the proposed test is conducted under various combinations of treatments under two factors. We assume that a proportion of π_m of test units are assigned to usage mode m, and we naturally have $\sum_{m=1}^{M}\pi_m = 1$. Further, under mode m, J levels of the continuous factor are specified for testing. In other words, the test plan is "balanced" with respect to the number of treatments in each level of the discrete factor. More discussions on this will be provided in Section 3.3. By denoting the levels of the continuous factor in mode m by $x_{m1}, \ldots, x_{mJ}$, where $x_{m1} < x_{m2} < \ldots < x_{mJ}$, and the respective proportion of test units by $\pi_{m1}, \ldots, \pi_{mJ}$, the ADT planning can be illustrated by Fig. 1.

Additional assumptions regarding the ADT planning are given as follows:

- The total number of test units is fixed and is denoted by N.
- The inspection intervals are identical under different treatments and we denote the interval by $\Delta\tau$.
- The total number of inspections per test unit is fixed at K, which implies that the test lasts for a duration of $K\Delta\tau$.

Proposition 3. *To estimate the parameters in model (2), at least one test unit has to be assigned to each level of the discrete factor, i.e., $\pi_m > 0$ for $m = 1, \ldots, M$.*

The statement is intuitive as any $\pi_m = 0$ will make β_m and γ_m inestimable in the model. The proposition guarantees that the test has exactly $M \times J$ treatments.

3.2. Two types of planning schemes

To enhance the practical generality of the proposed model, we put forward two types of planning schemes: planning with minimum test treatments, by which we call the "constrained optimal planning", and the "global optimal planning". Prior to zooming into details, we discuss some related practical issues in reliability tests. First, accelerated tests typically require a certain number of test chambers to create elevated stresses. For the battery example discussed in the paper, the variation in environmental temperature is mostly realized by chambers. Second, there is usually a critical limit on the test duration. Manufacturers would spend more costs induced by test chambers and energy consumption to save time. Therefore, experiments for different treatments need to be conducted at the same time, which implies that the test chambers have to be sufficient to fulfill the experimental design. Considering the aforementioned issues, some manufacturers may wish to plan reliability tests that require fewer test chambers to reduce related costs. For the rechargeable battery example, the control of the continuous temperature needs test chambers while to alter the categorical mode factor does not, which implies that the total number of treatments in the continuous factor determines the number of necessary test chambers. In this sense, we introduce the following constraint to the problem: $x_{mj} = x_{m'j}$ for any $m \neq m'$ and $j = 1, \ldots, J$. The constraint manages to limit the number of levels of the continuous factor at J. In this sense, we construct the problem of constrained optimal planning.

For notational convenience, we use Ω to integrally represent the EPRR under different scenarios, thus the estimated Ω can be summarized as follows:

$$\hat{\Omega} = \begin{cases} \widehat{\mathrm{EPRR}}_0(L), & \text{for fixed return threshold (Model 0),} \\ \widehat{\mathrm{EPRR}}_1(l_{\min}, L_D), & \text{for random return threshold (exact, Model 1),} \\ \widehat{\mathrm{EPRR}}_2(l_{\min}, L_D), & \text{for random return threshold (approximate, Model 2).} \end{cases} \tag{12}$$

Note that we will use Model 0, Model 1 and Model 2 to denote the three scenarios hereafter. An underlying concern in $\hat{\Omega}$ emerges, that is, under any model the value of EPRR is in the range from 0 and 1, and it tends to be small (typically smaller than 20%) for common products. To minimize the asymptotic variance of $\hat{\Omega}$ implicitly treats it as a normal distributed random variable, which is inappropriate for random variables with bounded support as this brings concerns to the uncertainty quantification of the estimators. To overcome the issue, we utilize the well adopted logit model to transform $\hat{\Omega}$ to a random variable with infinite support. The logit function creates a map of probability values from (0,1) to $(-\infty, \infty)$ (Cramer, 2003). Specifically, a logit function of a probability p is given by $\mathrm{logit}(p) = \log(p/(1-p))$, where $p/(1-p)$ is the odds, i.e., the probability of success divided by the probability of failure. Analogously, we transform the current $\hat{\Omega}$ into a revised version as

follows:

$$\hat{\Omega} = \begin{cases} \text{logit}(\widehat{\text{EPRR}}_0(L)), & \text{for fixed return threshold (Model 0),} \\ \text{logit}(\widehat{\text{EPRR}}_1(l_{\min}, L_D)), & \text{for random return threshold, (exact, Model 1),} \\ \text{logit}(\widehat{\text{EPRR}}_2(l_{\min}, L_D)), & \text{for random return threshold (approximate, Model 2),} \end{cases} \tag{13}$$

so that we can then minimize the asymptotic variance of $\hat{\Omega}$. To plan a constrained test, the following problem needs to be solved to find the optimal plan $\boldsymbol{\xi}^{\dagger}$:

$$\begin{aligned} &\text{maximize} - \text{Avar}(\hat{\Omega}; \boldsymbol{\xi}) \\ &\text{subject to} \sum_{m=1}^{M}\sum_{j=1}^{J} \pi_{mj} = 1; \\ &\quad x_{mj} = x_{m'j} \text{ for any } m \neq m' \text{ and } j = 1, \ldots, J; \\ &\quad 0 \leq x_{mj} \leq 1 \text{ for any } m = 1, \ldots, M \text{ and } j = 1, \ldots, J. \end{aligned} \tag{14}$$

The other planning scheme is to remove the constraint on the number of treatments and strive to find the global optimal ADT plans. Straightforwardly, we formulate the problem as:

$$\begin{aligned} &\text{maximize} - \text{Avar}(\hat{\Omega}; \boldsymbol{\xi}) \\ &\text{subject to} \sum_{m=1}^{M}\sum_{j=1}^{J} \pi_{mj} = 1; \\ &\quad 0 \leq x_{mj} \leq 1 \text{ for any } m = 1, \ldots, M \text{ and } j = 1, \ldots, J, \end{aligned} \tag{15}$$

and we denote the corresponding optimal plan by $\boldsymbol{\xi}^{*}$. For simplicity in interpretation, we call $\boldsymbol{\xi}^{*}$ and $\boldsymbol{\xi}^{\dagger}$ the "global optimal plan" and the "constrained optimal plan" in the remainder of the paper.

Remark 2. The choice between $\boldsymbol{\xi}^{\dagger}$ and $\boldsymbol{\xi}^{*}$ depends on how the test planners regard the importance of absolute statistical performance and test convenience. Two possible scenarios exist. The first one is that the difference between $\text{Avar}(\hat{\Omega}; \boldsymbol{\xi}^{\dagger})$ and $\text{Avar}(\hat{\Omega}; \boldsymbol{\xi}^{*})$ is quite minor, and test planners may tend to conveniently carry out the test with $\boldsymbol{\xi}^{\dagger}$. The other scenario is that there is a sensible difference in the asymptotic variance. In this situation, test plan may need to figure out whether to choose a more convenience plan or not by comprehensively considering the tradeoff between estimation accuracy and test chamber cost, labor cost, etc.

The complexity in the objective functions in (14) and (15) makes it an onerous task to derive analytical solutions to the optimization problems. One may have to resort to numerical methods to solve for the optimal plans. Fortunately, under the ADT planning framework, the number of decision variables are generally small. Additionally, some statistical insights gleaned from the theories of optimal designs can be utilized to simplify our problem, which is discussed in detail in the following context.

3.3. General results and insights

Maximum likelihood estimation (MLE) plays a dominant role in reliability test data modeling owing to its appealing asymptotic properties. To this end, the test planning procedures usually hinge on the MLE framework. For test unit $i = 1, \ldots, N$, denote the experimental condition by $\boldsymbol{x}_i$, where $\boldsymbol{x}_i$ is governed by the optimal plan described in Section 3.2. Belonging to the exponential dispersion degradation models (Tseng & Lee, 2016), the Wiener degradation process features the property that the increments from two non-overlapping intervals are independent. Therefore, the degradation increments between $(k-1)\Delta\tau$ and $k\Delta\tau$, denoted by ΔY_{ik}, follow independent normal distributions as $\Delta Y_{ik} \sim \mathcal{N}(\mu(\boldsymbol{x}_i)\Delta\tau, \sigma^2\Delta\tau)$. Therefore, given observed data $\Delta y_{ik}, i = 1, \ldots, N, k = 1, \ldots, K$, the log-likelihood function is given by

$$\ell(\boldsymbol{\theta}|\text{data}) = \sum_{i=1}^{N}\sum_{k=1}^{K} \log\phi\left[\frac{\Delta y_{ik} - \mu(\boldsymbol{x}_i)\Delta\tau}{\sigma\sqrt{\Delta\tau}}\right]. \tag{16}$$

By maximizing (16), the MLE of $\boldsymbol{\theta}$ is obtained and denoted by $\hat{\boldsymbol{\theta}}$. Further, the following elaborations are put forward to quantify the uncertainty of $\hat{\Omega}$. Based on the results in Meeker et al. (1998) under a specific ADT plan $\boldsymbol{\xi}$ and objective EPRR under Ω, the asymptotic variance of $\hat{\Omega}$ can be approximated by:

$$\text{Avar}(\hat{\Omega}; \boldsymbol{\xi}) = \boldsymbol{H}_{\Omega}^{T}(\boldsymbol{\theta})\left[\mathbf{I}(\boldsymbol{\theta}; \boldsymbol{\xi})\right]^{-1}\boldsymbol{H}_{\Omega}(\boldsymbol{\theta}), \tag{17}$$

where $\boldsymbol{H}_{\Omega}$ is the vector of first derivatives of Ω with respect to each unknown parameters, i.e.,

$$\boldsymbol{H}_{\Omega}(\boldsymbol{\theta}) = \left(\frac{\partial\Omega}{\partial\beta_0}, \frac{\partial\Omega}{\partial\beta_1}, \ldots, \frac{\partial\Omega}{\partial\beta_M}, \frac{\partial\Omega}{\partial\sigma}, \frac{\partial\Omega}{\partial\gamma_2}, \ldots, \frac{\partial\Omega}{\partial\gamma_M}\right)^{T}.$$

and

$$\mathbf{I}(\boldsymbol{\theta}; \boldsymbol{\xi}) = \mathbb{E}\left[-\frac{\ell^2}{\partial\boldsymbol{\theta}\partial\boldsymbol{\theta}^{T}}\right] \tag{18}$$

is the Fisher information of $\boldsymbol{\theta}$ under plan $\boldsymbol{\xi}$. The forgoing analysis provides a consistent objective function for the problem of interest. Obviously, $\boldsymbol{H}(\boldsymbol{\theta})$ is an invariant of test plan $\boldsymbol{\xi}$, and the derivation of $\boldsymbol{H}(\boldsymbol{\theta})$ is trivial and thus omitted in the paper. Test plan only influences the Fisher information $\mathbf{I}(\boldsymbol{\theta}; \boldsymbol{\xi})$. A noteworthy point is that the Fisher information stays the same for the same test plan under different objective functions in the paper. Appendix B shows the detailed derivations of the Fisher information.

Lemma 1. *Under model 2, the optimal plan $\boldsymbol{\xi}$ has $M \times 2$ treatments, i.e., $J = 2$. The optimality can be verified by Theorem 3.*

The lemma can be easily justified by the fact that the number of regression parameters is $2M$ (as regression parameters include $\beta_0, \beta_1, \ldots, \beta_M$ and $\gamma_2, \ldots, \gamma_M)'$ (Shi, Escobar, & Meeker, 2009). As stated in Section 3.1, the plan is assumed to be balanced with equal J under each level of m, thus $J = 2$. Lemma 1 implies that under each level of m, the optimal ADT plan is a simple two-level design. Although the problem can be simplified a bit from the lemma, the analytical solver cannot be attained due to the complexity in the objective function. Numerical optimization is inevitable in solving the problem. A critical drawback of numerical methods is the difficulty in guaranteeing the global optimality. Owing to the advances in theories of optimal design, we can take advantage of the following theorem to verify the optimality of test plans.

Theorem 3 (General Equivalence Theorem)**.** *The following results apply to the problem described in (15):*

1. *The objective function $-\text{Avar}(\hat{\Omega}; \boldsymbol{\xi})$ is concave with respect to test plans. In other words, for any $0 < \alpha < 1$ and two different test plans $\boldsymbol{\xi}$ and $\boldsymbol{\zeta}$, we have*

$$-\text{Avar}(\hat{\Omega}; \alpha\boldsymbol{\xi} + (1-\alpha)\boldsymbol{\zeta}) > -\alpha\text{Avar}(\hat{\Omega}; \boldsymbol{\xi}) - (1-\alpha)\text{Avar}(\hat{\Omega}; \boldsymbol{\zeta}). \tag{19}$$

2. *The directional derivative, denoted by Λ, of the objective function at $\boldsymbol{\xi}$ at the direction of the alternative plan $\boldsymbol{\zeta}$, can be represented by*

$$\begin{aligned} \Lambda(\boldsymbol{\xi}, \boldsymbol{\zeta}) = \boldsymbol{H}_{\Omega}^{T}(\boldsymbol{\theta})\left[\mathbf{I}(\boldsymbol{\theta}; \boldsymbol{\xi})\right]^{-1}\mathbf{I}(\boldsymbol{\theta}; \boldsymbol{\zeta})\left[\mathbf{I}(\boldsymbol{\theta}; \boldsymbol{\xi})\right]^{-1} \\ \boldsymbol{H}_{\Omega}(\boldsymbol{\theta}) - \boldsymbol{H}_{\Omega}^{T}(\boldsymbol{\theta})\left[\mathbf{I}(\boldsymbol{\theta}; \boldsymbol{\xi})\right]^{-1}\boldsymbol{H}_{\Omega}(\boldsymbol{\theta}). \end{aligned} \tag{20}$$

3. *For any $a_i > 0$ where $\sum_i a_i = 1$, if we have a series of alternative plans $\boldsymbol{\zeta}_i$ and their convex combination $\sum_i a_i \boldsymbol{\zeta}_i$, the following equation holds under the directional derivative:*

$$\Lambda\left(\boldsymbol{\xi}, \sum_i a_i \boldsymbol{\zeta}_i\right) = \sum_i a_i \Lambda\left(\boldsymbol{\xi}, \boldsymbol{\zeta}_i\right). \tag{21}$$

If conditions 1–3 hold for the derivative function and test plans, then the following results follow immediately from Theorem 1 parts (i), (ii), (iii), and (c) from Whittle (1973):

(a) *By letting $\boldsymbol{\xi}_{\boldsymbol{x}}$ be the test plan that puts all the units at level $\boldsymbol{x}$, a test plan $\boldsymbol{\xi}^*$ is optimal if and only if $\sup_{\boldsymbol{x}} \Lambda(\boldsymbol{\xi}^*, \boldsymbol{\xi}_{\boldsymbol{x}}) = 0$.*
(b) *The stress levels $\boldsymbol{x}_l^*$ in the optimal plan is a subset of $\boldsymbol{x}$ that satisfies $\sup_{\boldsymbol{x}} \Lambda(\boldsymbol{\xi}^*, \boldsymbol{\xi}_{\boldsymbol{x}}) = 0$.*

One appealing advantage of the General Equivalence Theorem (GET) is that (20) can be easily evaluated by analytical means and the results serve as input to items (a) and (b) in the theorem to verify the optimality of test plans obtained via numerical methods. It is worth mentioning that the GET can only be applied to the problem in (15) because the problem in (14) is actually to find a *suboptimal* test plan under additional constraints.

3.4. Compromise plans

In the presence of considerable uncertainty in the pilot model, compromise plans are usually preferable to enhance the robustness of the plan. The compromise plan usually contains extra stress levels that is analogous to adding center/side points to experimental designs (Del Castillo, 2007). The compromise test can be planned when preliminary data indicates abnormities in the residual analysis, and more general models can be estimated by the data generated by the compromise test. A common concern in the ADT planning is the appropriateness of the log-linear assumption in (2). Although the log-linear models are widely applied in ADT planning literature, the concern about two-level plans has been aroused soon after its proposal (Meeker & Escobar, 2015). For example, suppose that we are considering the following link function that can be possibly the true model rather than the one in (2):

$$\log \mu(x, m) = \begin{cases} \beta_0 + \beta_1 x + \beta_{11} x^2, & \text{if } m = 1 \\ \beta_0 + \beta_m x + \beta_{mm} x^2 + \gamma_m, & \text{if } m = 2, \ldots, M, \end{cases} \tag{22}$$

then a plan with $2M$ treatments will fail to estimate the quadratic parameters β_{11} and β_{mm} as the model involves $3M$ parameters. To overcome the shortcoming of the two-level plans, extra stress levels need to be inserted to the plans. Previous studies have set up some practical rules for three-level compromise ADT plans (Tseng & Lee, 2016) and it is a common practice to use a 10% or 20% rule to allocate test units to the extra stress level. Considering the uniqueness of the problem described in the paper, at a compromise level of $(100 \times \kappa)\%$, we solve the problem as follows:

$$\begin{aligned} \text{maximize} \quad & -\text{Avar}(\hat{\Omega}; \boldsymbol{\xi}) \\ \text{subject to} \quad & \sum_{m=1}^{M} \sum_{j=1}^{3} \pi_{mj} = 1; \\ & \sum_{m=1}^{M} \pi_{m2} = \kappa; \\ & \pi_{m2} > 0, \text{ for any } m = 1, \ldots, M; \\ & x_{m2} = (x_{m1} + x_{m3})/2 \text{ for any } m = 1, \ldots, M; \\ & 0 \le x_{mj} \le 1 \text{ for any } m{=}1, \ldots, M \text{ and } j{=}1, 2, 3. \end{aligned} \tag{23}$$

Analogously, the problem under the stress constraint is formulated as:

$$\begin{aligned} \text{maximize} \quad & -\text{Avar}(\hat{\Omega}; \boldsymbol{\xi}) \\ \text{subject to} \quad & \sum_{m=1}^{M} \sum_{j=1}^{3} \pi_{mj} = 1; \\ & \sum_{m=1}^{M} \pi_{m2} = \kappa; \\ & \pi_{m2} > 0, \text{ for any } m = 1, \ldots, M; \\ & x_{m2} = (x_{m1} + x_{m3})/2 \text{ for any } m = 1, \ldots, M; \\ & x_{mj} = x_{m'j} \text{ for any } m \ne m' \text{ and } j = 1, \ldots, J; \\ & 0 \le x_{mj} \le 1 \text{ for any } m{=}1, \ldots, M \text{ and } j{=}1, 2, 3. \end{aligned} \tag{24}$$

Note that κ denotes the total proportion of test units that are allocated to the extra "mid-stress-levels". The optimal rules to provide reasonable robustness are beyond the scope of the paper. More often than not, κ is set by a small proportion from 10% to 30% depending on the extent of compromise. A more scientific method to plan robust tests with respect to model misspecification is Bayesian planning (Insua, Ruggeri, Soyer, & Wilson, 2019). Since it is not the focus of the paper, we leave the Bayesian approaches for the problem as a future work.

4. Examples

4.1. Test planning for rechargeable batteries

In order to grab market share and reduce the cost induced by post-sales service, the lead acid rechargeable battery manufacturers improve the design of products frequently. On the one hand, battery design improvement intends to bring immediate performance enhancement that is sensible to customers. On the other, new technologies and designs may bring unknown risks to products, which could lead to high return rate in the future. The example discussed in the section is from one of the top-ranked acid rechargeable battery manufacturers based in China. From January to August 2017, the external losses (mainly because of the products return) of the company is around $11,000,000, accounting for 71% of the quality and reliability related cost. In general, battery manufacturers pay great efforts to conduct various tests to validate the reliability of products that are used by customers in various modes. For batteries, a degradation experiment for newly developed batteries takes up to half a year in normal conditions. In this situation, many products cannot be adequately verified under the strategy of bringing products to market faster than competitors. This has motivated the managerial team and engineers to seek for a scientific approach to degradation test planning that incorporates the consumers usage modes in the market.

Based on domain knowledge and previous experience of reliability tests, engineers believe that environmental temperature significantly affects the lead-acid batterys capacity. Specifically, the battery capacity degrades faster as the temperature increases from 25 °C to 65 °C. The failure mode can change when the temperature is higher than 65 °C, thus the maximum test temperature is set at 65 °C. Another factor that affects the reliability of batteries is the charging mode. The proposed model in (2) can well satisfy the requirements to plan tests for the batteries. To facilitate further elaborations, we standardize the temperature factor into the range from 0 to 1, where $x = 0$ and $x = 1$ indicate the normal usage temperature and maximum allowed temperature. In the example, we assume that $x = 0$ and $x = 1$ correspond to 25 °C and 65 °C, respectively. Let TK_i denote the thermodynamic temperature under the ith stress level, then according to the Arrhenius model

Table 1
Preliminary settings for the test.

Description	Notation	Value
Number of test units	N	200
Inspection interval	$\Delta\tau$	5
Number of inspections (for each test unit)	K	20
Maximum allowable temperature	$T_{\max}$	65 °C
Warranty period	τ_W	730 days
Deterministic failure threshold	L	5
Minimum returnable threshold	$l_{\min}$	4.5
Random delay return level	L_D	$\sim$ Gamma(1, 0.5)

(Meeker et al., 1998), x_i can be standardized as:

$$x_i = \frac{1/TK_{\min} - 1/TK_i}{1/TK_{\min} - 1/TK_{\max}}, \tag{25}$$

where $TK_{\min}$ and $TK_{\max}$ are equal to 298.15 Kelvin and 348.15 Kelvin, respectively. For illustrative purposes, we assume that three charging modes are considered. Planning settings and parameters are listed in Tables 1 and 2, respectively. It is noted that we set $l_{\min} = 4.5$ and $L_D \sim \text{Gamma}(1, 0.5)$ to describe the randomness in return level. In this sense, we keep the mean of $l_{\min} + L_D$ the same as L. Nevertheless, the median and mode of $l_{\min} + L_D$ are both smaller than L, which implies that more products tend to be returned earlier when the return threshold is random. We will conduct more sensitivity analysis with respect to L_D in Section 4.5.

Tables 3 and 4 exhibit the global optimal plan and constrained optimal plan, respectively, under the three proposed models. From Table 3 it is observed that the optimal stress levels are the same under three proposed methods. Specifically, the lower stress level x^*_{m1} is higher for $m = 2$ while is lower for $m = 3$. Interestingly, even though we assign the highest proportion to the mode $m = 1$, the optimal plans assign most test units to $m = 3$. A possible reason behind the phenomenon is that products under mode $m = 3$ are more likely to be returned by the customers due to its higher degradation rate as γ_3 is greater. By comparing the global optimal plans under the three models, we find that when the return level is random, slightly more test units tend to be allocated to $m = 1$. Additionally, the minimum asymptotic variance of $\hat{\Omega}$ is smaller in the presence of randomness in return level at the current setting. In general, the optimal plans under Model 1 and Model 2 are reasonably close, yet the approximation embedded in Model 2 leads to incorrectly lower asymptotic variance of the value of interest than the true value.

In contrast to the global optimal plans, the constrained optimal plans under three models suggest different optimal lower stress levels and a slightly different allocation scheme. Naturally, the minimum asymptotic variances under constrained optimal plans are higher than those under global optimal plans, while only slight margins are witnessed from the results. The current parameter settings yield true values of Ω under Models 0, 1 and 2 to be -2.20, -1.88 and -1.78, respectively. Therefore, the constrained optimal plans have provided relatively small asymptotic variances in comparison to the absolute values of true Ω's. Due to the fact that the global plans seem to outperform the constrained plans only by a small margin, the test plans may choose the constrained optimal plans that save more test resources as the preferable schemes. We can also observe that all the optimal higher stress levels (x^*_{m2}) are equal to 1, implying that the optimal plan always utilizes the highest allowed temperature to fully take advantage of the feasible experimental region.

4.2. Verification of optimality

The optimality of test plans can be readily verified by the results in Theorem 3. The derivative functions of global optimal plans at different values of x are plotted in Fig. 2 under different values of m and proposed models. The plot of derivative functions indicates that the plans in Table 3 are global optimal under the three models. To contrast, we exhibit the plots for the constrained optimal plans in Fig. 3, in which we can notice that the derivative values are greater than 0 at particular values of x. Therefore, in view of global optimality, the constrained test plans are suboptimal. Further, the results in the plots also verify Lemma 1 by demonstrating that a two-level plan for each m formulates the global optimal plan.

4.3. Simulation study

To demonstrate the efficiency of the large-sample approximation employed in the model, Monte Carlo simulation is conducted. We simulate large numbers of test data sets according to the settings in Tables 1 and 2 and the optimal test plans in Tables 3 and 4. The number of simulated data sets under each test plan is 10,000. Table 5 depicts the average bias and standard error for each unknown parameter under various models, and in the last two rows, the sample variance computed from the simulated data (denoted by $\text{var}(\hat{\Omega})$) and the theoretical asymptotic variance of $\hat{\Omega}$ are compared. Generally, the accuracy of estimation is fairly high and we can observe a satisfactory consistency in $\text{var}(\hat{\Omega})$ and $\text{Avar}(\hat{\Omega})$ under each model. Taken together, for the settings in the example, the adoption of large-sample approximation is reasonable, which thereby validates the appropriateness of the optimal plans.

4.4. Compromise plans

Three-level compromise plans were introduced in Section 3.4 to improve the model robustness. For illustrative purposes, we set the total proportion of test units to the extra levels as 10%, i.e., $\kappa = 0.1$. The global optimal and constrained optimal compromise plans are listed in Tables 6 and 7, respectively. We define the "Relative Efficiency (RE)" of a test plan as follows:

$$\text{RE}(\boldsymbol{\xi}) = \begin{cases} \text{Avar}(\hat{\Omega}; \boldsymbol{\xi}^*)/\text{Avar}(\hat{\Omega}; \boldsymbol{\xi}), & \text{for global optimality,} \\ \text{Avar}(\hat{\Omega}; \boldsymbol{\xi}^\dagger)/\text{Avar}(\hat{\Omega}; \boldsymbol{\xi}), & \text{for constrained optimality.} \end{cases} \tag{26}$$

In this manner, a higher RE represents that the efficiency of a test plan is closer to the optimal. As shown in Table 6, the extra mid-level stress ranges from 0.67 to 0.75 under different m and models, and most units assigned to extra stress are allocated to $m = 2$. In comparison to the results in Table 3, the compromise plan is fairly close to the two-level optimal plans regardless of the extra stress level. Similarly, Table 7 exhibits analogous results. The reported high REs ranging from 0.95 to 0.98 indicate a very marginal loss of efficiency loss under the setting $\kappa = 0.1$.

Understandably, the increase in κ would increase the power to detect the lack-of-fit of the model, whereas it inevitably degrades the RE of a test plan. Thus, it is of interest to explore how the change in κ affects the REs of the compromise optimal plans. Figure 4 displays the values of RE under different scenarios when κ ranges from 0 to 0.4. The REs for the global compromise plans generally behave a near-linear reduction in the increase of κ, while there is a slight fluctuation around $\kappa = 0.2$ under Model 1 and Model 2. To contrast, the REs for the constrained compromise plans decreases relatively slower when κ increases from 0 to a small value, whereas the speed of decrease increases as κ increases to a relatively higher value. In general, the REs of constrained compromise plans are higher than those of global compromise plans under a same κ. The interesting result implies that the constrained compromise plans are more robust than the global ones when κ changes. Reasons behind this can be partially explained as follows.

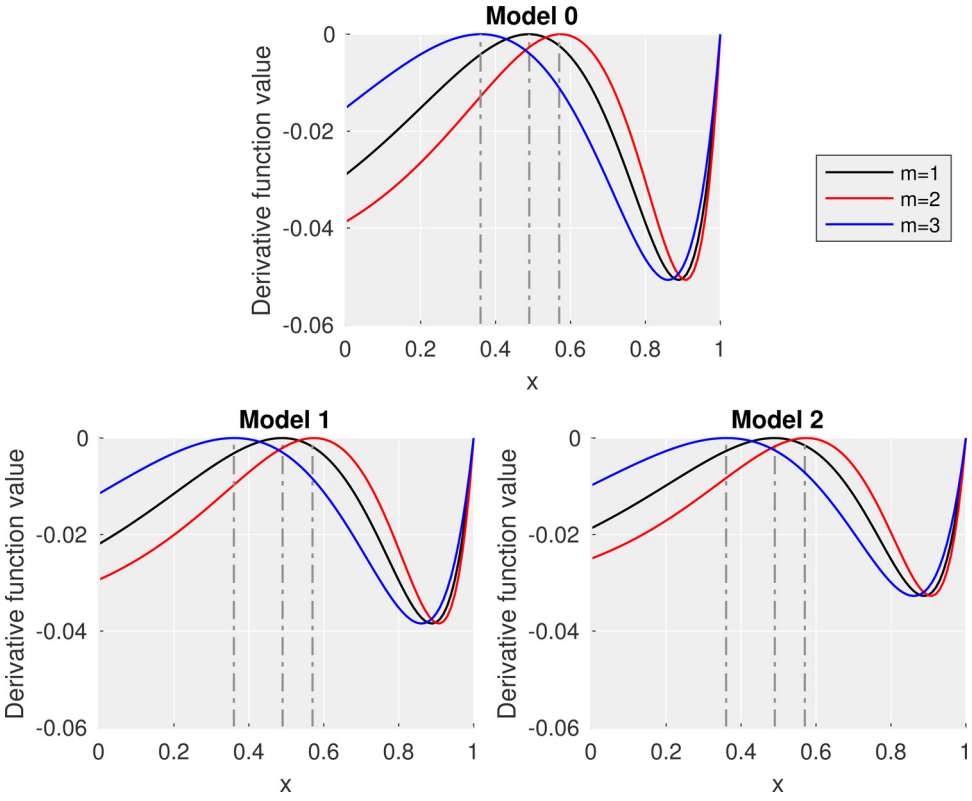

Fig. 2. Derivative functions against x under $\boldsymbol{\xi}^*$ for Model 0, 1 and 2.

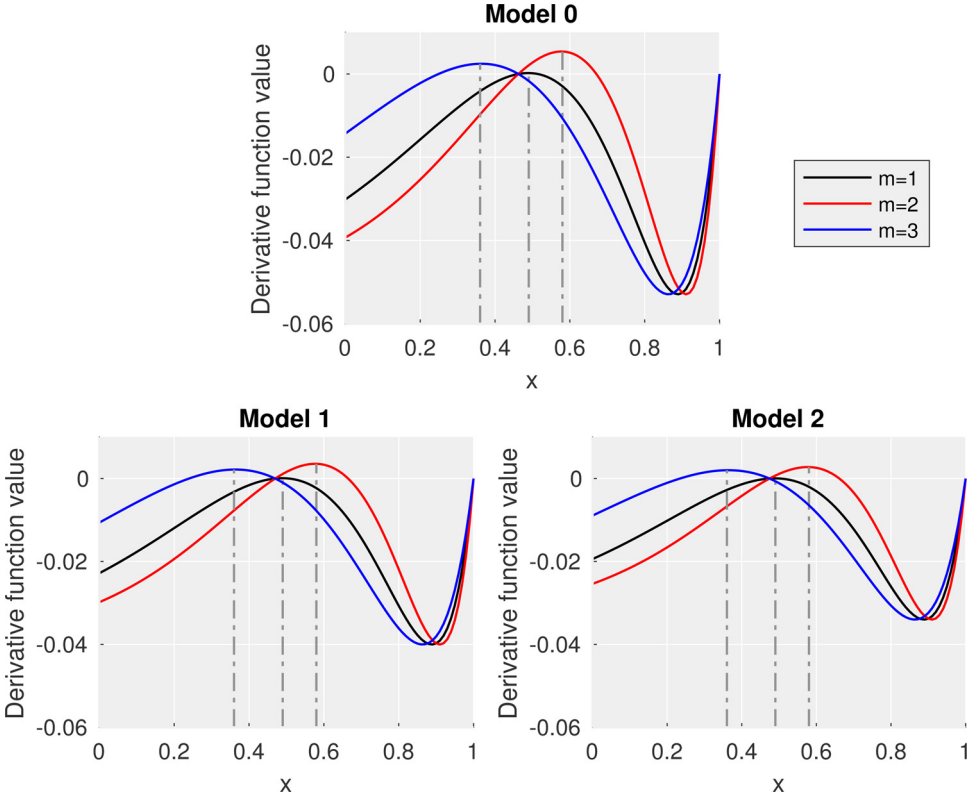

Fig. 3. Derivative functions against x under $\boldsymbol{\xi}^\dagger$ for Model 0, 1 and 2.

Table 2
Input parameters for test planning.

Parameter	$\boldsymbol{\theta}$							$\boldsymbol{\rho}$		
	β_0	β_1	β_2	β_3	σ	γ_2	γ_3	ρ_1	ρ_2	ρ_3
Value	-5.3	2.5	3.0	2.0	0.027	0.1	0.2	0.5	0.3	0.2

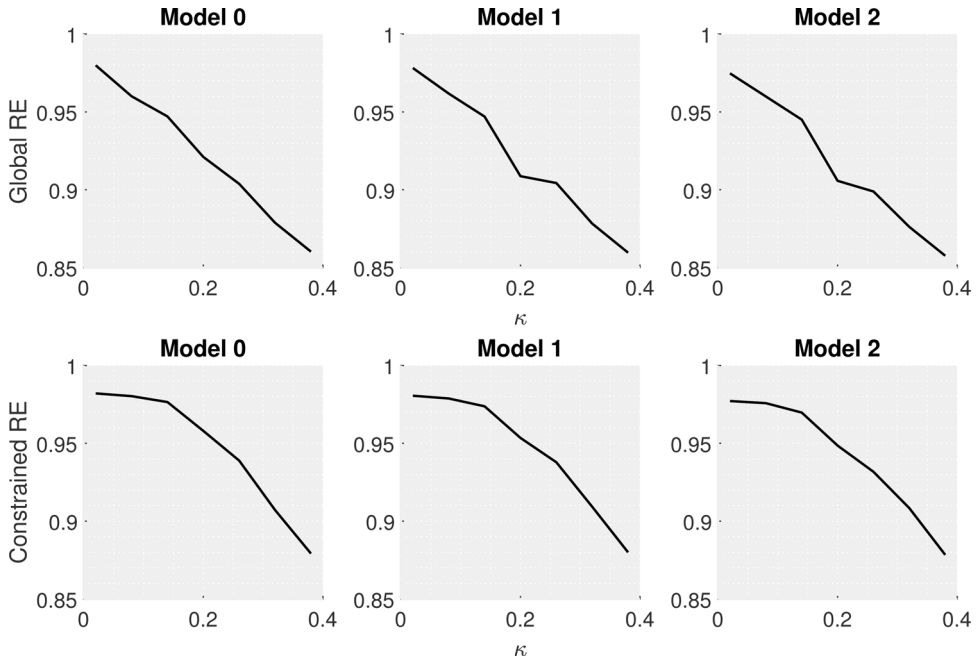

Fig. 4. RE of optimal compromise plans under different κ's.

Table 3
Global optimal plans.

Model	x_2	Optimal plan $\boldsymbol{\xi}^*$				Avar$\left[\hat{\Omega}; \boldsymbol{\xi}^*\right]$
		x^*_{m1} (temp°C)	x^*_{m2}(temp°C)	π^*_{m1}	π^*_{m2}	
0	$m=1$	0.489 (43.3)	1 (65.0)	0.22	0.03	0.0514
	$m=2$	0.574 (46.7)	1 (65.0)	0.22	0.03	
	$m=3$	0.361 (38.3)	1 (65.0)	0.45	0.05	
1	$m=1$	0.489 (43.3)	1 (65.0)	0.27	0.04	0.0388
	$m=2$	0.574 (46.7)	1 (65.0)	0.22	0.04	
	$m=3$	0.361 (38.3)	1 (65.0)	0.39	0.04	
2	$m=1$	0.489 (43.3)	1 (65.0)	0.31	0.04	0.0329
	$m=2$	0.574 (46.7)	1 (65.0)	0.22	0.03	
	$m=3$	0.361 (38.3)	1 (65.0)	0.36	0.04	

For global optimality, any alternative selection of stress levels, including the ones in the compromise ones, is worse than those in the global optimal plan. However, for the constrained optimality, the extra stress levels in the optimal compromise plans can to some extent compensate some efficiency incurred by the stress constraint, and keeps a higher RE for the constrained compromise plans. The aforementioned robustness is another advantage of the constrained plans in addition to the convenience of test implementation. Taken together, if the test planner wish to conduct a robust test plan under a limited number of test facilities, the constrained optimal compromise plans are preferable choices.

4.5. Sensitivity analysis

To further investigate the robustness of the test plans, we report on a series of sensitivity analysis. To be specific, three aspects of the model inputs are considered, that is, the unknown parameters $\boldsymbol{\theta}$, the probability model of usage mode $\boldsymbol{\rho}$ and the characteristics of the random return level $l_{\min} + L_D$.

Table 4
Constrained optimal plans.

Model	x_2	Optimal plan $\boldsymbol{\xi}^\dagger$				Avar$\left[\hat{\Omega}; \boldsymbol{\xi}^\dagger\right]$
		x^*_{m1} (temp°C)	x^*_{m2}(temp°C)	π^*_{m1}	π^*_{m2}	
0	$m=1$	0.462 (42.25)	1 (65.0)	0.22	0.03	0.0536
	$m=2$			0.23	0.02	
	$m=3$			0.43	0.07	
1	$m=1$	0.470 (42.55)	1 (65.0)	0.27	0.03	0.0404
	$m=2$			0.24	0.02	
	$m=3$			0.38	0.06	
2	$m=1$	0.474 (42.73)	1 (65.0)	0.30	0.04	0.0342
	$m=2$			0.24	0.02	
	$m=3$			0.34	0.06	

Table 5
Mean bias and standard error of unknown parameters and variance of $\hat{\Omega}$.

	Global optimal			Optimal under constrained x		
	Model 0	Model 1	Model 2	Model 0	Model 1	Model 2
bias($\hat{\beta}_0$)	-0.00100	-0.00116	0.00013	-0.00086	-0.00045	-0.00068
se($\hat{\beta}_0$)	0.04949	0.04459	0.04260	0.04996	0.04578	0.04340
bias($\hat{\beta}_1$)	0.00099	0.00094	-0.00021	0.00061	0.00035	0.00050
se($\hat{\beta}_1$)	0.05813	0.05307	0.05034	0.05944	0.05406	0.05053
bias($\hat{\beta}_2$)	-0.00005	0.00049	-0.00010	-0.00059	-0.00006	-0.00094
se($\hat{\beta}_2$)	0.03903	0.03768	0.03836	0.04131	0.03855	0.03920
bias($\hat{\beta}_3$)	0.00035	0.00067	-0.00025	0.00082	0.00053	0.00000
se($\hat{\beta}_3$)	0.04759	0.05012	0.05385	0.04636	0.04880	0.05239
bias($\hat{\sigma}$)	-0.00002	-0.00002	-0.00002	-0.00002	-0.00002	-0.00003
se($\hat{\sigma}$)	0.00030	0.00031	0.00031	0.00030	0.00030	0.00030
bias($\hat{\gamma}_2$)	0.00085	0.00056	-0.00012	0.00098	0.00064	0.00136
se($\hat{\gamma}_2$)	0.06027	0.05603	0.05419	0.06121	0.05694	0.05562
bias($\hat{\gamma}_3$)	0.00058	0.00039	-0.00010	0.00018	0.00011	0.00068
se($\hat{\gamma}_3$)	0.06256	0.05862	0.05921	0.06353	0.06071	0.06013
var($\hat{\Omega}$)	0.0513	0.0382	0.0339	0.0533	0.0400	0.0347
Avar($\hat{\Omega}$)	0.0514	0.0388	0.0329	0.0536	0.0404	0.0342

Table 6
Global optimal compromise plans under $\kappa = 0.1$.

Model	x_2	Optimal plan $\boldsymbol{\xi}_c^*$						Avar$\left[\hat{\Omega}; \boldsymbol{\xi}_c^*\right]$	RE
		x_{m1}^*	x_{m2}^*	x_{m3}^*	π_{m1}^*	π_{m2}^*	π_{m3}^*		
0	1	0.480 (42.97)	0.740 (53.61)	1 (65.0)	0.21	0.01	0.03	0.0538	0.955
	2	0.494 (43.50)	0.747 (53.90)	1 (65.0)	0.15	0.08	0.04		
	3	0.356 (38.11)	0.678 (51.00)	1 (65.0)	0.43	0.01	0.04		
1	1	0.482 (43.03)	0.741 (53.65)	1 (65.0)	0.26	0.01	0.04	0.0406	0.956
	2	0.497 (43.62)	0.748 (53.96)	1 (65.0)	0.15	0.08	0.04		
	3	0.355 (38.08)	0.678 (50.98)	1 (65.0)	0.37	0.01	0.04		
2	1	0.483 (43.06)	0.741 (53.65)	1 (65.0)	0.29	0.01	0.04	0.0345	0.954
	2	0.498 (43.66)	0.749 (53.98)	1 (65.0)	0.16	0.08	0.04		
	3	0.355 (38.05)	0.677 (50.97)	1 (65.0)	0.34	0.01	0.03		

Table 7
Constrained optimal compromise plans under $\kappa = 0.1$.

Model	x_2	Optimal plan $\boldsymbol{\xi}_c^\dagger$						Avar$\left[\hat{\Omega}; \boldsymbol{\xi}_c^\dagger\right]$	RE
		x_{m1}^*	x_{m2}^*	x_{m3}^*	π_{m1}^*	π_{m2}^*	π_{m3}^*		
0	1	0.425 (40.77)	0.712 (52.43)	1 (65.0)	0.21	0.01	0.02	0.0548	0.978
	2				0.15	0.08	0.04		
	3				0.42	0.01	0.06		
1	1	0.434 (41.14)	0.717 (52.63)	1 (65.0)	0.26	0.01	0.03	0.0414	0.976
	2				0.15	0.08	0.04		
	3				0.37	0.01	0.05		
2	1	0.440 (41.36)	0.720 (52.75)	1 (65.0)	0.29	0.01	0.03	0.0351	0.974
	2				0.15	0.08	0.04		
	3				0.33	0.01	0.05		

Sensitivity with respect to the unknown parameters

The parameter vector $\boldsymbol{\theta}$ is usually provided by experienced experts before a test is planned. Sometimes, the unknown parameters in $\boldsymbol{\theta}$ are misspecified due to the lack of prior knowledge about the product to be tested. To this end, we explore how the marginal changes in each parameter can affect the efficiency of the resulted optimal test plans. We add more details to the RE proposed in (26) as follows:

$$\mathrm{RE}(\boldsymbol{\xi}, \boldsymbol{\theta}) = \begin{cases} \mathrm{Avar}(\hat{\Omega}; \boldsymbol{\xi}^*, \boldsymbol{\theta})/\mathrm{Avar}(\hat{\Omega}; \boldsymbol{\xi}, \boldsymbol{\theta}), & \text{for global optimality,} \\ \mathrm{Avar}(\hat{\Omega}; \boldsymbol{\xi}^\dagger, \boldsymbol{\theta})/\mathrm{Avar}(\hat{\Omega}; \boldsymbol{\xi}, \boldsymbol{\theta}), & \text{for constrained optimality.} \end{cases} \tag{27}$$

As with the equation above, we define all the REs under true parameters. In this sense, we evaluate the true asymptotic variances of Ω of the test plan optimized under misspecified parameters and compare them with the true asymptotic variances. Further, we utilize the true covariance matrix of $\hat{\Omega}$, which is the inverse of $\mathbf{I}(\boldsymbol{\theta})$, under test plan $\boldsymbol{\xi}^*$ under Model 0 in Table 3 to quantify the uncertainties of each parameter in $\boldsymbol{\theta}$. Specifically, we compute the standard deviation of the unknown parameters as follows:

$$\sigma_{\theta_i} = \sqrt{\left[(\mathbf{I}(\boldsymbol{\theta}))^{-1}\right]_{ii}}, \tag{28}$$

for $i = 1, \ldots, 7$, where $[\cdot]_{ii}$ denotes the ith diagonal element of a matrix. Then, we explore how the change in each parameter by $\pm\sigma_{\theta_i}$, $\pm 2\sigma_{\theta_i}$ and $\pm 3\sigma_{\theta_i}$ influences the REs and the results are displayed in Table 8. We highlight the REs that are smaller than 0.9 by bold text in the table. As observed, the REs are more sensitive to the change in parameters β_0, γ_2 and γ_3, which is understandable because these parameters determine the degradation models under the normal condition of x_1, i.e., $x_1 = 0$. Specifically, the RE decreases considerably when β_0 is over-specified or γ_2 and γ_3 are under-specified. Thus, test planners should avoid such cases to improve the robustness of the test plans. In general, most REs listed in the table are quite high and this indicates adequate robustness of the test plans in the current settings.

Table 8
The RE of optimal test plans under misspecified parameters. (Values smaller than 0.9 are **bold**).

Model	θ_i	Global optimal						Constrained optimal					
		$-3\sigma_{\theta_i}$	$-2\sigma_{\theta_i}$	$-1\sigma_{\theta_i}$	$+1\sigma_{\theta_i}$	$+2\sigma_{\theta_i}$	$+3\sigma_{\theta_i}$	$-3\sigma_{\theta_i}$	$-2\sigma_{\theta_i}$	$-1\sigma_{\theta_i}$	$+1\sigma_{\theta_i}$	$+2\sigma_{\theta}$	$+3\sigma_{\theta_i}$
0	β_0	0.950	0.973	0.992	0.988	0.946	**0.862**	0.949	0.972	0.992	0.988	0.945	**0.861**
	β_1	0.996	0.998	1.000	1.000	0.998	0.996	0.998	0.999	1.000	1.000	0.999	0.998
	β_2	0.999	0.999	1.000	1.000	0.999	0.999	0.999	1.000	1.000	1.000	1.000	0.999
	β_3	0.995	0.998	1.000	1.000	0.998	0.995	0.996	0.998	1.000	1.000	0.998	0.996
	σ	0.998	0.999	1.000	1.000	0.999	0.999	0.998	0.999	1.000	1.000	0.999	0.998
	γ_2	**0.647**	**0.839**	0.962	0.975	0.928	**0.895**	**0.635**	**0.832**	0.960	0.974	0.925	**0.891**
	γ_3	**0.700**	**0.878**	0.976	0.991	0.988	0.999	**0.693**	**0.874**	0.975	0.991	0.987	0.999
1	β_0	0.950	0.972	0.990	0.988	0.953	**0.887**	0.943	0.965	0.983	0.981	0.946	**0.880**
	β_1	0.993	0.996	0.997	0.997	0.996	0.993	0.988	0.990	0.990	0.990	0.990	0.988
	β_2	0.996	0.997	0.998	0.998	0.997	0.996	0.990	0.990	0.991	0.991	0.990	0.990
	β_3	0.993	0.996	0.997	0.997	0.996	0.993	0.988	0.989	0.990	0.990	0.989	0.988
	σ	0.997	0.997	0.998	0.998	0.997	0.997	0.990	0.990	0.991	0.991	0.990	0.990
	γ_2	**0.755**	**0.895**	0.975	0.984	0.961	0.950	**0.742**	**0.885**	0.967	0.977	0.953	0.941
	γ_3	**0.818**	0.933	0.986	0.995	0.996	0.996	**0.808**	0.924	0.979	0.988	0.989	0.989
2	β_0	0.940	0.970	0.991	0.990	0.968	0.935	0.940	0.970	0.991	0.991	0.968	0.935
	β_1	0.994	0.996	0.998	0.998	0.996	0.994	0.996	0.997	0.999	0.999	0.997	0.996
	β_2	0.997	0.998	0.998	0.998	0.998	0.997	0.998	0.998	0.999	0.999	0.998	0.998
	β_3	0.994	0.997	0.998	0.998	0.997	0.995	0.996	0.998	0.999	0.999	0.998	0.996
	σ	0.998	0.998	0.998	0.998	0.998	0.998	0.999	0.999	0.999	0.999	0.999	0.999
	γ_2	**0.811**	0.925	0.984	0.991	0.979	0.971	**0.805**	0.923	0.983	0.991	0.978	0.971
	γ_3	**0.885**	0.962	0.993	0.997	0.996	0.998	**0.882**	0.961	0.993	0.997	0.997	0.999

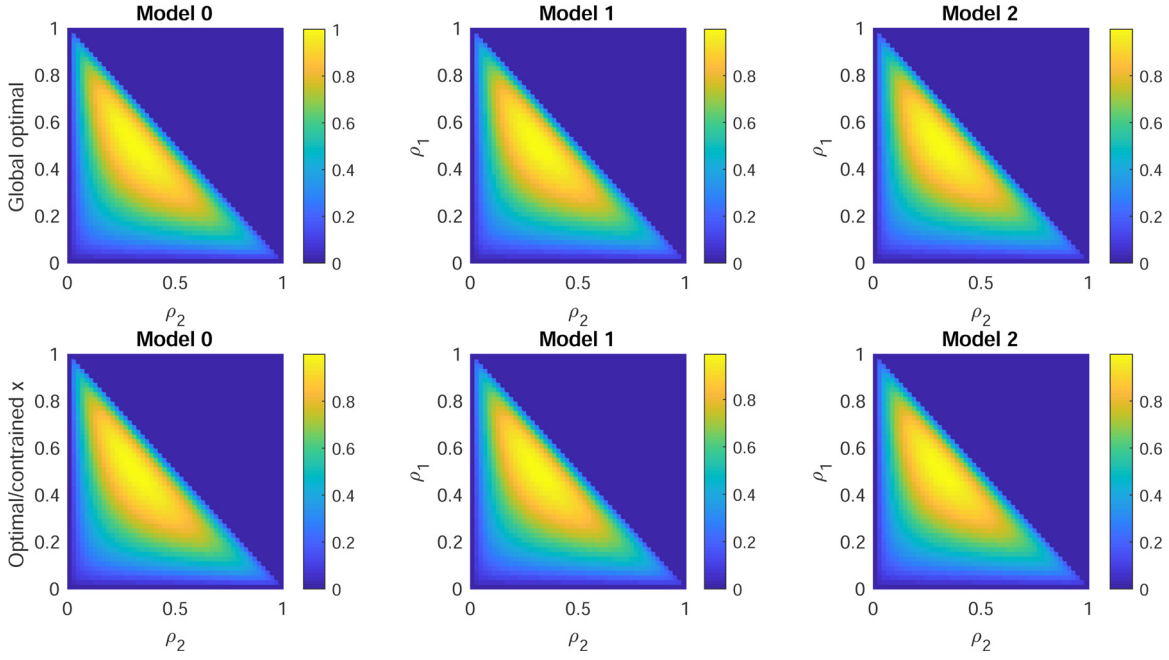

Fig. 5. Surface plot of RE under different combinations of ρ_1 and ρ_2.

Sensitivity with respect to probability model of usage modes

Apart from the unknown parameters, the test planner has to provide the probabilities of usage mode $\boldsymbol{\rho}$. Analogously, we use the RE defined under true $\boldsymbol{\rho}$ and compute them under misspecified $\boldsymbol{\rho}$. Fig. 5 displays the surface plot of RE when ρ_1 and ρ_2 take different values. We can see that the misspecification of $\boldsymbol{\theta}$ can possibly lead to very low REs, especially when ρ_1 and ρ_2 are specified as extreme values that are close to 0 or 1. When the specified $\boldsymbol{\rho}$ is fairly closer to the true $\boldsymbol{\rho}$, the RE can retain at a high level (≥ 0.8). The sensitivity analysis, in general, indicates the importance to specify $\boldsymbol{\rho}$ that is close to the true one. Test planners are suggested to collect adequate and reliable information on $\boldsymbol{\rho}$ to facilitate the test planning. Fortunately, in a particular industry, the probability model of usage modes of customers for similar products could be quite close and related information can be collected based on existing data and experiences.

Sensitivity with respect to the parameters in L_D

Next, we explore the influence of characteristics of the random return level $l_{\min} + L_D$ on the optimal test plans. Since the randomness of $l_{\min} + L_D$ completely lies in L_D, we evaluate the asymptotic variances under different settings of L_D, and the results are displayed in Table 9. We put forward two scenarios to keep the comparison consistent. In the first one, the mean of L_D is kept at 0.5, while in the second one the mode is kept at 0.5. Then, the variance of L_D is adjusted and the asymptotic variances as well as REs are compared. As a side note, we only adopt Model 1 to conduct the analysis. An interesting result observed from the table is that when the variances gets larger, the asymptotic variance of $\hat{\Omega}$ becomes smaller. The underlying reason can be that the gamma distribution is a right-skewed distribution, when the variance gets larger with a fixed mean or mode, the distribution will be more right skewed, which implies that a larger probability density when L_D

Table 9
The asymptotic variance of $\hat{\Omega}$ and RE under different settings of L_D.

L_D	var(L_D)	shape	scale	Global optimal		Constrained optimal	
				Avar$\left[\hat{\Omega};\boldsymbol{\xi}^*\right]$	RE	Avar$\left[\hat{\Omega};\boldsymbol{\xi}^\dagger\right]$	RE
Mean = 0.5	0.10	2.50	0.20	0.0436	0.8906	0.0454	0.8898
	0.25	1.00	0.50	0.0388	1.0000	0.0404	1.0000
	0.50	0.50	1.00	0.0358	1.0830	0.0372	1.0840
Mode = 0.5	0.10	4.27	0.15	0.0491	0.7905	0.0512	0.7891
	0.25	2.62	0.31	0.0472	0.8213	0.0492	0.8198
	0.50	2.00	0.50	0.0456	0.8498	0.0476	0.8484

is relatively small. It is understandable that when the realizations of $l_{\min}+L_D$ are smaller, the asymptotic variance of $\hat{\Omega}$ should be smaller as the extent of extrapolation is reduced. These results, in general, suggest that the determination of L_D can be quite important to plan the test and predict the return rate. Again, like $\boldsymbol{\rho}$, the determination of L_D can be aided by existing data and experiences.

5. Conclusions

This paper investigates the optimization of reliability tests for return rate prediction based on a prevailing degradation-failure model. The proposed model allows for the existence of multiple customer usage modes and random return level. We have given analytical forms of the return rate model and the large-sample approximation approach is employed to quantify the uncertainty of the estimated return rate. Two types of test plans, namely global optimal plans and constrained optimal plans, are put forward to satisfy different requirements of the decision maker. A real motivating example from the battery industry is analyzed to demonstrate the proposed methods. Our results have suggested the adoption of the constrained optimal plans that compromise limited statistical efficiency whereas simplify the test implementation and offer more robustness under compromise plans. Moreover, the sensitivity analysis emphasizes the importance of accurately determining the probabilities of customer usage modes.

It is of interest to extend the methods to scenarios with more complicated product return models. The heterogeneity in products and customer behaviors can be modeled in a more general manner. Moreover, for products subject to several stress factors, the model can be extended to incorporate multiple continuous and discrete factors. The adaption to products with multiple key components is also significant to manufacturers of more complex products. Bayesian approaches or nonparametric methods can be explored to plan similar reliability tests in the absence of reliable parameter settings and specification of the degradation model. Furthermore, the approaches to data analytics based on the test data can be of interest for more specific prediction of return rate.

Acknowledgments

The work is in part supported by the National Natural Science Foundation of China (72002149, 72032005, 71971181, 72002066) and in part by the Humanity and Social Science Youth Foundation of Ministry of Education of China (19YJC630117).

Appendix A. Technical proofs

Proof of Proposition 2 The idea behind Proposition 2 originates from the Taylor expansion. We can expand $\mathbb{E}_{L_D}[F_T(L_D)]$ as follows:

$$\mathbb{E}_{L_D}[F_T(L_D)] = F_T(\mu_{L_D}) + \sum_{n=2}^{\infty} \frac{F_T^{(n)}(\mu_{L_D})}{n!}\mathbb{E}\left[(L_D-\mu_{L_D})^n\right].$$

If we adopt the second-order approximation, then

$$\begin{aligned}\mathbb{E}_{L_D}[F_T(L_D)] &\approx F_T(\mu_{L_D}) + \frac{1}{2}F_T^{(2)}(\mu_{L_D})\mathbb{E}\left[(L_D-\mu_{L_D})^2\right]\\ &= F_T(\mu_{L_D}) + \frac{1}{2}F_T^{(2)}(\mu_{L_D})\mathrm{var}(L_D),\end{aligned}$$

which yields (10). The derivation of (11) is trivial and thus omitted. □

A1. Proof of Theorem 1

To justify the results (a) and (b) in the general equivalence theorem, we need to prove conditions 1–3 in the theorem. To start with, (19) is proved as follows. We first have

$$\begin{aligned}&-\mathrm{Avar}(\hat{\Omega};\alpha\boldsymbol{\xi}+(1-\alpha)\boldsymbol{\zeta}) + \alpha\mathrm{Avar}(\hat{\Omega};\boldsymbol{\xi}) + (1-\alpha)\mathrm{Avar}(\hat{\Omega};\boldsymbol{\zeta})\\ &= \boldsymbol{H}_\Omega^T(\boldsymbol{\theta})\Big\{\alpha\left[\mathbf{I}(\boldsymbol{\theta};\boldsymbol{\xi})\right]^{-1} + (1-\alpha)\left[\mathbf{I}(\boldsymbol{\theta};\boldsymbol{\zeta})\right]^{-1}\\ &\quad -\left[\mathbf{I}(\boldsymbol{\theta};\alpha\boldsymbol{\xi}+(1-\alpha)\boldsymbol{\zeta})\right]^{-1}\Big\}\boldsymbol{H}_\Omega(\boldsymbol{\theta}).\end{aligned} \tag{B.3}$$

Further, due to the fact that $\mathbf{I}(\boldsymbol{\theta};\alpha\boldsymbol{\xi}+(1-\alpha)\boldsymbol{\zeta}) = \alpha\mathbf{I}(\boldsymbol{\theta};\boldsymbol{\xi}) + (1-\alpha)\mathbf{I}(\boldsymbol{\theta};\boldsymbol{\zeta})$, we have

$$\begin{aligned}&\alpha\left[\mathbf{I}(\boldsymbol{\theta};\boldsymbol{\xi})\right]^{-1} + (1-\alpha)\left[\mathbf{I}(\boldsymbol{\theta};\boldsymbol{\zeta})\right]^{-1} - \left[\mathbf{I}(\boldsymbol{\theta};\alpha\boldsymbol{\xi}+(1-\alpha)\boldsymbol{\zeta})\right]^{-1}\\ &= \alpha\left[\mathbf{I}(\boldsymbol{\theta};\boldsymbol{\xi})\right]^{-1} + (1-\alpha)\left[\mathbf{I}(\boldsymbol{\theta};\boldsymbol{\zeta})\right]^{-1}\\ &\quad -\left[\alpha\mathbf{I}(\boldsymbol{\theta};\boldsymbol{\xi}) + (1-\alpha)\mathbf{I}(\boldsymbol{\theta};\boldsymbol{\zeta})\right]^{-1},\end{aligned}$$

which is positive definite following the results in Section V-C in Xiao & Ye (2016). Since $\alpha\mathbf{I}(\boldsymbol{\theta};\boldsymbol{\xi}) + (1-\alpha)\mathbf{I}(\boldsymbol{\theta};\boldsymbol{\zeta})$ is positive definite, then (B.3) is greater than zero for any $\boldsymbol{H}_\Omega(\boldsymbol{\theta}) \neq \mathbf{0}$, which completes the proof of (19). Afterward, according to the definition of the derivative function in the GET, we have

$$\Lambda(\boldsymbol{\xi},\boldsymbol{\zeta}) = \lim_{\delta\to 0^+}\frac{-\mathrm{Avar}(\hat{\Omega};(1-\delta)\boldsymbol{\xi}+\delta\boldsymbol{\zeta}) + \mathrm{Avar}(\hat{\Omega};\boldsymbol{\xi})}{\delta}. \tag{B.4}$$

Now apply the l'Hôpital's rule to (B.4), and we get

$$\begin{aligned}&\lim_{\delta\to 0^+}\frac{-\mathrm{Avar}(\hat{\Omega};(1-\delta)\boldsymbol{\xi}+\delta\boldsymbol{\zeta}) + \mathrm{Avar}(\hat{\Omega};\boldsymbol{\xi})}{\delta}\\ &= \lim_{\delta\to 0^+}\frac{-\partial\mathrm{Avar}(\hat{\Omega};(1-\delta)\boldsymbol{\xi}+\delta\boldsymbol{\zeta})}{\partial\delta}\\ &= \lim_{\delta\to 0^+}\frac{-\partial\boldsymbol{H}_\Omega^T(\boldsymbol{\theta})\left[\mathbf{I}(\boldsymbol{\theta};(1-\delta)\boldsymbol{\xi}+\delta\boldsymbol{\zeta})\right]^{-1}\boldsymbol{H}_\Omega(\boldsymbol{\theta})}{\partial\delta}\\ &\text{(Split Fisher information)}\\ &= \lim_{\delta\to 0^+}\frac{-\partial\boldsymbol{H}_\Omega^T(\boldsymbol{\theta})\left[(1-\delta)\mathbf{I}(\boldsymbol{\theta};\boldsymbol{\xi}) + \delta\mathbf{I}(\boldsymbol{\theta};\boldsymbol{\zeta})\right]^{-1}\boldsymbol{H}_\Omega(\boldsymbol{\theta})}{\partial\delta}\\ &\text{(Apply the chain rule)}\\ &= \lim_{\delta\to 0^+}\boldsymbol{H}_\Omega^T(\boldsymbol{\theta})\left[(1-\delta)\mathbf{I}(\boldsymbol{\theta};\boldsymbol{\xi}) + \delta\mathbf{I}(\boldsymbol{\theta};\boldsymbol{\zeta})\right]^{-1}\left[-\mathbf{I}(\boldsymbol{\theta};\boldsymbol{\xi}) + \mathbf{I}(\boldsymbol{\theta};\boldsymbol{\zeta})\right]\\ &\times\left[(1-\delta)\mathbf{I}(\boldsymbol{\theta};\boldsymbol{\xi}) + \delta\mathbf{I}(\boldsymbol{\theta};\boldsymbol{\zeta})\right]^{-1}\boldsymbol{H}_\Omega(\boldsymbol{\theta})\end{aligned}$$

$$= \boldsymbol{H}_{\Omega}^{T}(\boldsymbol{\theta})\left[\mathbf{I}(\boldsymbol{\theta};\boldsymbol{\xi})\right]^{-1}\left[-\mathbf{I}(\boldsymbol{\theta};\boldsymbol{\xi})+\mathbf{I}(\boldsymbol{\theta};\boldsymbol{\zeta})\right]\left[\mathbf{I}(\boldsymbol{\theta};\boldsymbol{\xi})\right]^{-1}\boldsymbol{H}_{\Omega}(\boldsymbol{\theta})$$
$$= \boldsymbol{H}_{\Omega}^{T}(\boldsymbol{\theta})\left[\mathbf{I}(\boldsymbol{\theta};\boldsymbol{\xi})\right]^{-1}\mathbf{I}(\boldsymbol{\theta};\boldsymbol{\zeta})\left[\mathbf{I}(\boldsymbol{\theta};\boldsymbol{\xi})\right]^{-1}\boldsymbol{H}_{\Omega}(\boldsymbol{\theta})$$
$$-\boldsymbol{H}_{\Omega}^{T}(\boldsymbol{\theta})\left[\mathbf{I}(\boldsymbol{\theta};\boldsymbol{\xi})\right]^{-1}\boldsymbol{H}_{\Omega}(\boldsymbol{\theta}),$$

and thus this completes the proof of (20). The fact that $\mathbf{I}\left(\boldsymbol{\theta};\sum_i a_i\boldsymbol{\zeta}_i\right)=\sum_i a_i\mathbf{I}\left(\boldsymbol{\theta};\boldsymbol{\zeta}_i\right)$ together with (20) can prove (21) after simple mathematical manipulations. The proofs above have ensured that conditions 1–3, then the GET can be well applied to the problem.

Appendix B. Expression of the Fisher information

According to (18), the elements in the matrix can be expressed by

$$\mathbb{E}\left[-\frac{\ell^2}{\partial\beta_0^2}\right]=\frac{NK\Delta\tau}{\sigma^2}\sum_{m=1}^{M}\sum_{j=1}^{J}\pi_{mj}\left[\mu(x_{mj},m)\right]^2,$$
$$\mathbb{E}\left[-\frac{\ell^2}{\partial\beta_0\partial\beta_m}\right]=\mathbb{E}\left[-\frac{\ell^2}{\partial\beta_m\partial\beta_0}\right]$$
$$=\frac{NK\Delta\tau}{\sigma^2}\sum_{j=1}^{J}\pi_{mj}\left[\mu(x_{mj},m)\right]^2x_{mj},\ \text{for } m=1,\ldots,M,$$
$$\mathbb{E}\left[-\frac{\ell^2}{\partial\beta_m^2}\right]=\frac{NK\Delta\tau}{\sigma^2}\sum_{j=1}^{J}\pi_{mj}\left[\mu(x_{mj},m)\right]^2x_{mj}^2,\ \text{for } m=1,\ldots,M,$$
$$\mathbb{E}\left[-\frac{\ell^2}{\partial\sigma^2}\right]=\frac{2NK}{\sigma^2},$$
$$\mathbb{E}\left[-\frac{\ell^2}{\partial\gamma_m^2}\right]=\frac{NK\Delta\tau}{\sigma^2}\sum_{j=1}^{J}\pi_{mj}\left[\mu(x_{mj},m)\right]^2,\ \text{for } m=2,\ldots,M,$$
$$\mathbb{E}\left[-\frac{\ell^2}{\partial\gamma_m\partial\beta_0}\right]=\mathbb{E}\left[-\frac{\ell^2}{\partial\beta_0\partial\gamma_m}\right]$$
$$=\frac{NK\Delta\tau}{\sigma^2}\sum_{j=1}^{J}\pi_{mj}\left[\mu(x_{mj},m)\right]^2,\ \text{for } m=2,\ldots,M.,$$
$$\mathbb{E}\left[-\frac{\ell^2}{\partial\gamma_m\partial\beta_m}\right]=\mathbb{E}\left[-\frac{\ell^2}{\partial\beta_m\partial\gamma_m}\right]$$
$$=\frac{NK\Delta\tau}{\sigma^2}\sum_{j=1}^{J}\pi_{mj}\left[\mu(x_{mj},m)\right]^2x_{mj},\ \text{for } m=2,\ldots,M.$$

and other elements all equal to zero.

References

Cheng, S., Li, B., Yuan, Z., Zhang, F., & Liu, J. (2016). Development of a lifetime prediction model for lithium thionyl chloride batteries based on an accelerated degradation test. *Microelectronics Reliability, 65*, 274–279. https://doi.org/10.1016/j.microrel.2016.07.152.

Chhikara, R. (1988). *The inverse Gaussian distribution: Theory: methodology, and applications*: vol. 95. CRC Press.

Cramer, J. S. (2003). *The origins and development of the logit model* (pp. 149–157)). Cambridge University Press.

Darghouth, M., Ait-kadi, D., & Chelbi, A. (2017). Joint optimization of design, warranty and price for products sold with maintenance service contracts. *Reliability Engineering & System Safety, 165*, 197–208. https://doi.org/10.1016/j.ress.2017.03.033.

Del Castillo, E. (2007). *Process optimization: A statistical approach*: vol. 105. Springer Science & Business Media.

Escobar, L. A., & Meeker, W. Q. (2006). A review of accelerated test models. *Statistical Science, 21*(4), 552–577. https://doi.org/10.1214/088342306000000321.

Fang, G., Pan, R., & Stufken, J. (2020). Optimal setting of test conditions and allocation of test units for accelerated degradation tests with two stress variables. *IEEE Transactions on Reliability*. https://doi.org/10.1109/TR.2020.2995333. in press

Fang, G., Pan, R., & Wang, Y. (2022). Inverse Gaussian processes with correlated random effects for multivariate degradation modeling. *European Journal of Operational Research*. https://doi.org/10.1016/j.ejor.2021.10.049.

Gil-Pelaez, J. (1951). Note on the inversion theorem. *Biometrika, 38*(3–4), 481–482.

Hsu, N.-j., Tseng, S.-t., & Chen, M.-w. (2015). Adaptive warranty prediction for highly reliable products. *IEEE Transactions on Reliability, 64*(3), 1057–1067. https://doi.org/10.1109/TR.2015.2427153.

Hu, C.-H., Lee, M.-Y., & Tang, J. (2015). Optimum step-stress accelerated degradation test for Wiener degradation process under constraints. *European Journal of Operational Research, 241*(2), 412–421. https://doi.org/10.1016/j.ejor.2014.09.003.

Hua, C., Zhang, Q., Xu, G., Zhang, Y., & Xu, T. (2013). Performance reliability estimation method based on adaptive failure threshold. *Mechanical Systems and Signal Processing, 36*(2), 505–519. https://doi.org/10.1016/j.ymssp.2012.10.019.

Insua, D. R., Ruggeri, F., Soyer, R., & Wilson, S. (2019). Advances in Bayesian decision making in reliability. *European Journal of Operational Research*. https://doi.org/10.1016/j.ejor.2019.03.018.

Lee, I. C., Tseng, S. T., & Hong, Y. (2020). Global planning of accelerated degradation tests based on exponential dispersion degradation models. *Naval Research Logistics, 67*(6), 469–483. https://doi.org/10.1002/nav.21923.

Li, T., He, S., & Zhao, X. (2022). Optimal warranty policy design for deteriorating products with random failure threshold. *Reliability Engineering & System Safety, 218*, 108142. https://doi.org/10.1016/j.ress.2021.108142.

Li, X., Rezvanizaniani, M., Ge, Z., Abuali, M., & Lee, J. (2015). Bayesian optimal design of step stress accelerated degradation testing. *Journal of Systems Engineering and Electronics, 26*(3), 502–513. https://doi.org/10.1109/JSEE.2015.00058.

Li, X.-Y., Wu, J.-P., Ma, H.-G., Li, X., & Kang, R. (2018). A random fuzzy accelerated degradation model and statistical analysis. *IEEE Transactions on Fuzzy Systems, 26*(3), 1638–1650. https://doi.org/10.1109/TFUZZ.2017.2738607.

Lim, H., & Yum, B.-J. (2011). Optimal design of accelerated degradation tests based on Wiener process models. *Journal of Applied Statistics, 38*(2), 309–325. https://doi.org/10.1080/02664760903406488.

Meeker, W. Q., & Escobar, L. A. (2015). A review of recent research and current issues in AT. *International Statistical Review, 61*(1), 147–168. https://doi.org/10.2307/1403600.

Meeker, W. Q., Escobar, L. A., & Lu, C. J. (1998). Accelerated degradation tests: Modeling and analysis. *Technometrics, 40*(2), 89–99. https://doi.org/10.1080/00401706.1998.10485191.

Sarada, Y., & Shenbagam, R. (2021). Optimization of a repairable deteriorating system subject to random threshold failure using preventive repair and stochastic lead time. *Reliability Engineering and System Safety, 205*, 107229. https://doi.org/10.1016/j.ress.2020.107229.

Shi, Y., Escobar, L. A., & Meeker, W. Q. (2009). Accelerated destructive degradation test planning. *Technometrics, 51*(1), 1–13.

Si, X. S. (2015). An adaptive prognostic approach via nonlinear degradation modeling: Application to battery data. *IEEE Transactions on Industrial Electronics, 62*(8), 5082–5096. https://doi.org/10.1109/TIE.2015.2393840.

Thomas, E. V., Bloom, I., Christophersen, J. P., & Battaglia, V. S. (2008). Statistical methodology for predicting the life of lithium-ion cells via accelerated degradation testing. *Journal of Power Sources, 184*(1), 312–317. https://doi.org/10.1016/j.jpowsour.2008.06.017.

Tian, J., Xiong, R., & Shen, W. (2020). State-of-health estimation based on differential temperature for lithium ion batteries. *IEEE Transactions on Power Electronics, 35*(10), 10363–10373. https://doi.org/10.1109/TPEL.2020.2978493.

Tseng, S.-T., Hsu, N.-J., & Lin, Y.-C. (2016). Joint modeling of laboratory and field data with application to warranty prediction for highly reliable products. *IIE Transactions, 48*(8), 710–719. https://doi.org/10.1080/0740817X.2015.1133941.

Tseng, S.-T., & Lee, I.-C. (2016). Optimum allocation rule for accelerated degradation tests with a class of exponential-dispersion degradation models. *Technometrics, 58*(2), 244–254. https://doi.org/10.1080/00401706.2015.1033109.

Walsh, G., Albrecht, A. K., Kunz, W., & Hofacker, C. F. (2016). Relationship between online retailers' reputation and product returns. *British Journal of Management, 27*(1), 3–20. https://doi.org/10.1111/1467-8551.12120.

Wang, P., & Coit, D. (2007). Reliability and degradation modeling with random or uncertain failure threshold. In *2007 Proceedings - annual reliability and maintainability sympsoium* (pp. 392–397). IEEE. https://doi.org/10.1109/RAMS.2007.328107. http://ieeexplore.ieee.org/document/4126383/

Wang, X., Wang, B. X., Hong, Y., & Jiang, P. H. (2021). Degradation data analysis based on gamma process with random effects. *European Journal of Operational Research, 292*(3), 1200–1208. https://doi.org/10.1016/j.ejor.2020.11.036.

Whittle, P. (1973). Some general points in the theory of optimal experimental design. *Journal of the Royal Statistical Society: Series B (Methodological), 35*(1), 123–130.

Xiao, X., & Ye, Z. (2016). Optimal design for destructive degradation tests with random initial degradation values using the Wiener process. *IEEE Transactions on Reliability, 65*(3), 1327–1342.

Yang, G. (2010). Accelerated life test plans for predicting warranty cost. *IEEE Transactions on Reliability, 59*(4), 628–634. https://doi.org/10.1109/TR.2010.2085550. http://ieeexplore.ieee.org/lpdocs/epic03/wrapper.htm?arnumber=5613969

Ye, Z.-S., & Chen, N. (2014). The inverse Gaussian process as a degradation model. *Technometrics, 56*(3), 302–311. https://doi.org/10.1080/00401706.2013.830074.

Ye, Z.-S., & Xie, M. (2015). Stochastic modelling and analysis of degradation for highly reliable products. *Applied Stochastic Models in Business and Industry, 31*(1), 16–32. https://doi.org/10.1002/asmb.2063.

Zhai, Q., & Ye, Z.-S. (2017). RUL prediction of deteriorating products using an adaptive Wiener process model. *IEEE Transactions on Industrial Informatics, 13*(6), 2911–2921. https://doi.org/10.1109/TII.2017.2684821.

Zhang, Y., & Meeker, W. Q. (2006). Bayesian methods for planning accelerated life tests. *Technometrics, 48*(1), 49–60. https://doi.org/10.1198/004017005000000373.

Zhang, Z., Si, X., Hu, C., & Lei, Y. (2018). Degradation data analysis and remain-

ing useful life estimation: A review on Wiener-process-based methods. *European Journal of Operational Research, 271*(3), 775–796. https://doi.org/10.1016/j.ejor.2018.02.033.

Zhao, X., He, S., & Xie, M. (2018). Utilizing experimental degradation data for warranty cost optimization under imperfect repair. *Reliability Engineering & System Safety, 177*, 108–119. https://doi.org/10.1016/j.ress.2018.05.002.

Zhao, X., & Xie, M. (2017). Using accelerated life tests data to predict warranty cost under imperfect repair. *Computers & Industrial Engineering, 107*, 223–234. https://doi.org/10.1016/j.cie.2017.03.021.

Zhu, J., Dewi Darma, M. S., Knapp, M., Sørensen, D. R., Heere, M., Fang, Q., … Ehrenberg, H. (2020). Investigation of lithium-ion battery degradation mechanisms by combining differential voltage analysis and alternating current impedance. *Journal of Power Sources, 448*, 28–30. https://doi.org/10.1016/j.jpowsour.2019.227575.